Article:

Research

Author for correspondence:
William J. Parnell
e-mail: william.parnell@manchester.ac.uk

A unified framework for linear thermo-visco-elastic wave propagation including the effects of stress-relaxation

Erik García Neefjes[1], David Nigro[2], Artur L. Gower[3], Raphaël C. Assier[1], Valerie J. Pinfield[4] and William J. Parnell[1]

[1]Department of Mathematics, University of Manchester, Oxford Road, Manchester M13 9PL, UK
[2]Thales UK, 350 Longwater Avenue Green Park, Reading RG2 6GF, UK
[3]Department of Mechanical Engineering, University of Sheffield, Sheffield, UK
[4]Department of Chemical Engineering, Loughborough University, Loughborough LE11 3TU, UK

EGN, 0000-0001-7114-2944; RCA, 0000-0001-9848-3482;
WJP , 0000-0002-3676-9466

We present a unified framework for the study of wave propagation in homogeneous linear thermo-visco-elastic (TVE) continua, starting from conservation laws. In free-space such media admit two thermo-compressional modes and a shear mode. We provide asymptotic approximations to the corresponding wavenumbers which facilitate the understanding of dispersion of these modes, and consider common solids and fluids as well as soft materials where creep compliance and stress relaxation are important. We further illustrate how commonly used simpler acoustic/elastic dissipative theories can be derived via particular limits of this framework. Consequently, our framework allows us to: (i) simultaneously model interfaces involving both fluids and solids and (ii) easily quantify the influence of thermal or viscous losses in a given configuration of interest. As an example, the general framework is applied

THE ROYAL SOCIETY
PUBLISHING

to the canonical problem of scattering from an interface between two TVE half spaces in perfect contact. To illustrate, we provide results for fluid–solid interfaces involving air, water, steel and rubber, paying particular attention to the effects of stress relaxation.

1. Introduction

Even under small deformations, complex continua exhibit a variety of constitutive effects over a broad range of frequencies, associated with their atomistic, molecular or mesoscopic properties. In the field of continuum mechanics, it has become commonplace to label a material either as *fluid* or *solid* and even when viscoelastic, for reasons of model simplification, there is a tendency to specify a medium as a viscoelastic *fluid* or viscoelastic *solid*. This matter is however made more complex when considering wave propagation in the medium over a wide range of frequencies and temperatures. Polymers are an exemplary example; they are fluid-like at low frequencies and solid-like at high frequencies and they take on similar properties as a (reciprocal) function of temperature [1,2]. The shear modulus of a polymeric material can vary by several orders of magnitude after transitioning through the glass-transition frequency/temperature [3,4].

Assuming specific material behaviour can be helpful to limit the number of parameters that have to be measured experimentally, but it can also, unintentionally, lead to additional complexities. For example, consider two *homogeneous* continua coupled at an interface, with the first being an *acoustic* medium, such that only compressional (longitudinal) waves propagate, while the second is an *elastic* medium which supports both shear (transverse) and compressional waves and displacement is vectorial [5]. Coupling the boundary conditions for acoustic and elastic waves can be awkward. This is especially true when it is important to include thermo-viscous effects [5,6]. A unified framework, as we present here, simplifies the calculations as there is no need to develop separate models (i.e. one for the acoustic and the other for the elastic), and types of boundary conditions.

In the context of thermo-visco-acoustics, effective boundary conditions have been devised to simplify the problem [7] but when strong coupling occurs, this same approach cannot be employed. What follows are then rather ad-hoc approaches and often questionable approximations, particularly with regard to modelling in the time domain.

In more complex, inhomogeneous media or *metamaterials*, the frequency dependence can often be very strong due to inherent resonances associated with microstructure [8,9]. These resonances are often tuned to be strong at low frequencies, given that this is often the regime in which traditional materials cannot yield dispersive effects. However the frequency dependence is tuned by resonator size and geometry, and the material properties of the matrix medium.

Understanding the wave propagation characteristics of metamaterials is frequently achieved by employing asymptotic theories, which rely on specific scalings of the material property contrast [10,11]. If this dependence changes with frequency then the entire theory underpinning these materials could be described as unstable. And the kinds of materials involved in high contrast resonance *are* precisely materials that would possess strong frequency dependence [12].

One may argue that experiments at fixed frequencies can be fitted to a theory with certain fixed parameters, whether one considers a metamaterial or a simple, homogeneous medium. This is certainly the case and this approach has been employed very successfully in the past [13,14]. However, one may reasonably ask what happens when we change frequency, or design a resonator in the same matrix material to act at a different frequency, or even more reasonably what happens in the time domain? In all of these cases, of crucial importance is the ability to model the material's behaviour properly in the frequency domain. It appears uncomfortable from both a practical and scientific perspective to fit different parameters to the behaviour over a broad range of frequencies. It is certainly more beneficial to bring forth a theoretical framework that can accommodate such dependence. Kelvin–Voigt visco-elasticity has been used with some success, but this theory does not accommodate stress relaxation, which is critically important in polymers,

when they undergo their glass transition, considered in either frequency or temperature space. Although for most materials this transition seems to occur in the lower frequency regime, one of the crucial aspects is that it affects both the real and imaginary part of the particular modulus [15], whereas Kelvin–Voigt models only capture the latter.

In the present article, we return to the fundamentals of linear continuum mechanics and present a general, unified framework with which to model a variety of TVE materials of interest, with the specific interest in modelling how they couple at interfaces. We discuss Kelvin–Voigt visco-elasticity and the standard linear models that extend this to incorporate stress relaxation. The same governing equations are used in any domain, without any need to identify the medium as a fluid, solid, viscoelastic or otherwise. Needless to say parameters are required, but this means that *a priori*, all that is needed is the identification of values that identify the medium as linear TVE, thus allowing one to model a vast range of important materials.

Over time the scientific community has developed a range of terms for specific media, e.g. *visco-acoustic*, *viscoelastic*, *thermoelastic*, etc. where certain physical effects are neglected. These are certainly useful and helpful because in many cases the neglected effects are not important. Here we also provide the asymptotic framework with which one can switch between these theories. In many cases, it is straightforward and we simply set specific constants to zero, meaning that a lack of coupling arises. However, in some cases, one must be careful in the manner by which the theory is simplified, as we discuss.

In §2, we begin with the conservation equations of homogeneous TVE materials, and describe local (in time) thermo-visco-elasticity before moving onto the more general non-local models that incorporate stress relaxation. These models are defined in the frequency domain and we consider Prony series that permit frequency dependence of material properties [16]. In §3, we go on to describe useful and appropriate asymptotic limits of the theory of thermo-visco-elasticity. Section 4 covers the application of the various theories to the canonical problem of wave reflection from an interface between two continua, with the effects of coupling being illustrated and in particular the effects of relaxation on the frequency-dependent transmission and reflection. We close in §5 with conclusions.

2. Modelling linear thermo-visco-elastic media

(a) Governing equations

Our starting point is the classical set of conservation laws of linear continuum mechanics: conservation of mass, momentum and energy, together with the Clausius–Duhem inequality [17]

$$\dot{\rho} + \rho \nabla \cdot \dot{\mathbf{u}} = 0, \tag{2.1a}$$

$$\rho \ddot{\mathbf{u}} = \nabla \cdot \boldsymbol{\sigma} + \rho \mathbf{G}, \tag{2.1b}$$

$$\rho \dot{\mathcal{E}} + \nabla \cdot \mathbf{q} = \boldsymbol{\sigma} : \dot{\varepsilon} + \rho B \tag{2.1c}$$

and

$$\rho T \dot{\mathfrak{s}} + \nabla \cdot \mathbf{q} \geq \rho B + \frac{\mathbf{q} \cdot \nabla \mathbf{T}}{T}, \tag{2.1d}$$

where notation is summarized in table 1, and the symmetry of the Cauchy stress tensor $\boldsymbol{\sigma} = \boldsymbol{\sigma}^T$ arises due to conservation of angular momentum.

(b) Local (in time) thermo-visco-elasticity

We assume that all constitutive models considered are local in space. We begin with the simplest (local) dependence on time, where we introduce the Helmholtz free energy per unit mass [18]

$$\Psi(t) \equiv \Psi(\varepsilon(t), T(t)) = \mathcal{E}(t) - T(t)\mathfrak{s}(t). \tag{2.2}$$

Table 1. Thermo-viscous parameters and other quantities that appear in the general TVE model. By the 'ambient' value of a quantity, we refer to its value prior to deformation, i.e. in the undeformed configuration which we assume to be still.

notation	
time derivative	$\dot{\circ} = \partial \circ / \partial t$
gradient operator	$\nabla \circ = \partial \circ / \partial x_i$
Laplacian operator	$\Delta \circ = \nabla \cdot \nabla \circ$
tensor contraction	$\boldsymbol{A} : \boldsymbol{B} = A_{ij} B_{ij}$
matrix trace and matrix transpose	$\mathrm{tr}(\circ)$ and $\circ^T$
Fourier component	$\circ = \mathrm{Re}\,\{\hat{\circ} e^{-i\omega t}\}$
complex conjugate	$\circ^*$
heaviside function	H
time average over wave period	$\langle \circ \rangle = (\omega/2\pi) \int_0^{2\pi/\omega} (\circ)\,dt$
three-dimensional identity tensor	$\boldsymbol{I}$

thermo-visco-elastic parameters		
parameters	unit(s)	symbols and definitions
continuum's displacement vector	m	u
infinitesimal strain tensor	—	$\varepsilon = (\nabla u + (\nabla u)^T)/2$
off-diagonal entries of the strain tensor	—	$\boldsymbol{e} = \varepsilon - \mathrm{tr}(\varepsilon)\boldsymbol{I}/3$
Cauchy stress tensor	N m^{-2}	$\boldsymbol{\sigma}$
off-diagonal entries of the stress tensor	N m^{-2}	$\boldsymbol{s} = \boldsymbol{\sigma} - \mathrm{tr}(\boldsymbol{\sigma})\boldsymbol{I}/3$
linear and angular frequency	Hz, rad s^{-1}	$f, \omega \quad \omega = 2\pi f$
classical (isothermal) Lamé coefficients	N m^{-2}	$\mu, \lambda > 0$
elastic bulk modulus (isothermal)	N m^{-2}	$K = \lambda + 2\mu/3$
elastic Poisson's ratio (isothermal)	—	ν
bulk and shear viscosity	N s m^{-2}	$\eta_K, \eta_\mu > 0, \quad \eta_\lambda = \eta_K - 2\eta_\mu/3$
viscosity parameter	N s m^{-2}	$\zeta = 2\eta_\mu + \eta_\lambda$
local in time complex Lamé quantities	N m^{-2}	$\hat{\lambda} = \lambda - i\omega\eta_\lambda, \ \hat{\mu} = \mu - i\omega\eta_\mu$
local in time complex bulk modulus	N m^{-2}	$\hat{K} = K - i\omega\eta_K$
thermal conductivity	W m^{-1} K^{-1}	$\mathscr{K}$
internal energy density per unit mass	N m kg^{-1}	$\mathcal{E}$
total and ambient temperature	K	T, T_0
non-dimensional temperature variation	—	$\theta = (T - T_0)/T_0$
total and ambient mass density	kg m^{-3}	ρ, ρ_0
total and ambient entropy per unit mass	N m kg^{-1} K^{-1}	$\mathfrak{s}, \mathfrak{s}_0$
specific heat at constant pressure/volume	J kg^{-1} K^{-1}	$c_p, c_v \ \rho_0(c_p - c_v) = \alpha^2 K T_0$
ratio of specific heats	—	$\gamma = c_p/c_v$
adiabatic/isothermal acoustic speed of sound	m s^{-1}	$c_A, c_{Iso} \quad c_A = \sqrt{\gamma}\, c_{Iso}$

(*Continued.*)

Using this in (2.1*c*), (2.1*d*) yields

$$\left(\boldsymbol{\sigma} - \rho \frac{\partial \Psi}{\partial \varepsilon}\right) : \dot{\varepsilon} - \left(\frac{\partial \Psi}{\partial T} + \mathfrak{s}\right)\rho \dot{T} - \frac{\mathbf{q} \cdot \nabla T}{T} \geq 0. \tag{2.3}$$

Table 1. (*Continued.*)

thermo-visco-elastic parameters		
parameters	unit(s)	symbols and definitions
coefficient of thermal expansion	K^{-1}	α
volumetric heat supply per unit mass	$N\,m\,kg^{-1}\,s^{-1}$	B
body force per unit mass	$N\,kg^{-1}$	G
Fourier-Stokes heat flux vector	$N\,m^{-1}\,s^{-1}$	q
total and ambient Helmholtz free energy per unit mass	$N\,m\,kg^{-1}$	Ψ, Ψ_0
thermal parameter	m^{-2}	L_ϕ
thermo-visco-elastic coupling quantity	—	L_θ
thermo-compressional wave-potentials and wavenumbers	m^2 and m^{-1}	φ, ϑ and k_φ, k_ϑ
pressure/shear wave-potentials and wavenumbers	m^2 and m^{-1}	ϕ, Φ and k_ϕ, k_Φ
temperature contributions	m^{-2}	$\mathscr{T}_\varphi$, $\mathscr{T}_\vartheta$
mechanical relaxation functions	$N\,m^{-2}$	$\mathcal{R}_1$, $\mathcal{R}_2$
thermo-mechanical relaxation function	$N\,m^{-2}\,K^{-1}$	$\mathcal{R}_3$
specific heat relaxation function	$J\,m^{-3}\,K^{-2}$	$\mathcal{R}_4$
energy flux vector per unit volume	$N\,m^{-1}\,s^{-1}$	J
total TVE energy per unit volume	$N\,m^{-2}$	$\mathcal{U}$
energy dissipation per unit time/volume	$N\,m^{-2}\,s^{-1}$	$\mathcal{D}$

We then adopt the approach of *Coleman-Noll* [19] and *Liu* [20] to yield further information; since (2.3) must hold for arbitrary deformations, the imposition of specific deformations permits conclusions to be deduced on functional form. A purely isothermal process ($\dot{T} = 0$, $\nabla T = \mathbf{0}$) and a process that involves no deformation but a change in uniform temperature, respectively, yields

$$\boldsymbol{\sigma}^{\mathrm{TE}} = \rho \frac{\partial \Psi}{\partial \varepsilon} \quad \text{and} \quad \mathfrak{s} = -\frac{\partial \Psi}{\partial T}, \tag{2.4}$$

where the superscript 'TE' refers to *thermo-elastic*. The conditions (2.4) are *sufficient* but not *necessary* to satisfy (2.3): one can include an additional visco-elastic (VE) contribution to the Cauchy stress, e.g. for isotropic media

$$\boldsymbol{\sigma} = \boldsymbol{\sigma}^{\mathrm{TE}} + \boldsymbol{\sigma}^{\mathrm{VE}} = \rho \frac{\partial \Psi}{\partial \varepsilon} + 2\eta_\mu \dot{\varepsilon} + \left(\eta_K - \frac{2}{3}\eta_\mu \right) \mathrm{tr}(\dot{\varepsilon})\boldsymbol{I}, \tag{2.5}$$

where the shear and bulk viscosities[1] (both constants here) satisfy $\eta_\mu > 0$, $\eta_\lambda = \eta_K - 2\eta_\mu/3 > 0$ and hence (2.5) also satisfies (2.3). The introduction of $\boldsymbol{\sigma}^{\mathrm{VE}}$ distinguishes the current local-in-time TVE models from the commonly employed classical TE models. However, the absence of stress rate terms in (2.5) is a strong restriction, since it fails to predict stress relaxation effects, which are important in many common materials such as polymers [21]. Incorporating stress rates results in models that we refer to as *non-local in time*, and this is the focus of §2c. We first describe the thermal constitutive models and then the associated equations that describe local-in-time TVE wave propagation.

---

[1]These terms are defined in several ways throughout the literature, our choice of η_K as the bulk viscosity matches the convention of the elastic bulk modulus.

We adopt Fourier's Law of heat conduction,

$$\mathbf{q} = -\mathscr{K}\nabla T, \tag{2.6}$$

where $\mathscr{K} > 0$ is the thermal conductivity of the material, whose positivity ensures that the last term in (2.3) is never negative. The form (2.6) is the simplest admissible choice, resulting in a parabolic diffusion equation (2.10) for which the thermal wave-speed is infinite. Thermal waves with finite velocity (e.g. Maxwell–Cattaneo heat waves) are obtained when introducing a thermal relaxation time which arises when taking into account the rate of heat flux vector in (2.6) [22,23].

At this stage, it only remains to determine the thermodynamically consistent form of Ψ. As shown in appendix A, for a (local) linear theory of thermo-visco-elasticity we obtain

$$\boldsymbol{\sigma} = 2\mu\varepsilon + 2\eta_\mu\dot{\boldsymbol{\varepsilon}} + (\lambda\mathrm{tr}(\varepsilon) + \eta_\lambda\mathrm{tr}(\dot{\varepsilon}) - \alpha K T_0\theta)\boldsymbol{I} \tag{2.7a}$$

and

$$\mathfrak{s} = \mathfrak{s}_0 + c_v\theta + \frac{\alpha K}{\rho_0}\mathrm{tr}(\varepsilon), \tag{2.7b}$$

where $\theta = (T - T_0)/T_0$ is the non-dimensional temperature difference, and $K = \lambda + 2\mu/3$ denotes the elastic bulk modulus measured at a state of constant temperature (i.e. isothermal like λ and μ, see appendix A). Note that by introducing the off-diagonal tensors $\boldsymbol{s}$ and $\boldsymbol{e}$ satisfying

$$\boldsymbol{s} = \boldsymbol{\sigma} - \frac{1}{3}\mathrm{tr}(\boldsymbol{\sigma})\boldsymbol{I} \quad \text{and} \quad \boldsymbol{e} = \varepsilon - \frac{1}{3}\mathrm{tr}(\varepsilon)\boldsymbol{I}, \tag{2.8}$$

we may deduce from (2.7a) that

$$\boldsymbol{s} = 2\mu\boldsymbol{e} + 2\eta_\mu\dot{\boldsymbol{e}}, \quad \mathrm{tr}(\boldsymbol{\sigma}) = 3[K\mathrm{tr}(\varepsilon) + \eta_K\mathrm{tr}(\dot{\boldsymbol{\varepsilon}}) - \alpha K T_0\theta]. \tag{2.9}$$

Substituting (2.2), (2.5) and (2.7b) into (2.1c) yields the energy equation

$$\mathscr{K}\Delta\theta - \rho_0 c_v\dot{\theta} = \alpha K\mathrm{tr}(\dot{\varepsilon}), \tag{2.10}$$

where we have assumed no external heat supply such that $B = 0$. Note that viscous effects are not explicit in (2.10) since they are quadratic in $\dot{\varepsilon}$, and hence at this order the energy is analogous to that of linear thermo-elasticity [18]. Finally for convenience, we write

$$\rho_0(\gamma - 1) = \frac{\alpha^2 K T_0}{c_v}, \tag{2.11}$$

where $\gamma = c_p/c_v$ denotes the ratio of specific heats. Equation (2.11) is a classical conserved quantity in thermo-elasticity (see appendix A). It is useful in practice since for solids c_v is difficult to measure as opposed to c_p. As we see shortly it plays an important role when considering the thermo-visco-acoustic (TVA) limit. Finally, we show in electronic supplementary material, section SM1 that for this model we can obtain the *energy conservation–dissipation corollary*

$$\nabla \cdot \mathbf{J} + \frac{1}{2}\dot{\mathcal{U}} = -\mathcal{D}, \quad \begin{cases} \mathbf{J} = -(\boldsymbol{\sigma}^{\mathrm{TVE}}\dot{\mathbf{u}} + T_0\theta\mathscr{K}\nabla\theta), \\ \mathcal{U} = \rho_0|\dot{\mathbf{u}}|^2 + \rho_0 T_0 c_v\theta^2 + 2\mu|\varepsilon|^2 + \lambda(\mathrm{tr}\varepsilon)^2, \\ \mathcal{D} = T_0\mathscr{K}|\nabla\theta|^2 + 2\eta_\mu|\dot{\varepsilon}|^2 + \eta_\lambda(\mathrm{tr}\dot{\varepsilon})^2, \end{cases} \tag{2.12}$$

where $\mathbf{J}$ represents the energy flux vector, $\mathcal{D}$ the energy dissipation and $\mathcal{U}$ the total TVE energy. Note that $\mathcal{D} \geq 0$, so that a non-zero temperature gradient and strain rate always dissipates energy. Similar results are given for visco-elasticity in [24, p. 20] and for thermo-elasticity in [25].

(i) Frequency domain decomposition for the local-in-time equations

We now assume time-harmonic propagation of the form $\{\mathbf{u}, \theta, \boldsymbol{\sigma}\}(\mathbf{x}, t) = \mathrm{Re}\{\{\hat{\mathbf{u}}, \hat{\theta}, \hat{\boldsymbol{\sigma}}\}(\mathbf{x})\,\mathrm{e}^{-\mathrm{i}\omega t}\}$ and define the complex-valued (Kelvin–Voigt like) Lamé parameters

$$\hat{\lambda} = \lambda - \mathrm{i}\omega\eta_\lambda \quad \text{and} \quad \hat{\mu} = \mu - \mathrm{i}\omega\eta_\mu, \tag{2.13}$$

so that with (2.13) we can write the time-harmonic Cauchy stress (2.7a) as

$$\hat{\boldsymbol{\sigma}} = (\hat{\lambda}\nabla \cdot \hat{\mathbf{u}} - \alpha K T_0 \hat{\theta})\boldsymbol{I} + \hat{\mu}(\nabla\hat{\mathbf{u}} + (\nabla\hat{\mathbf{u}})^T), \tag{2.14}$$

or equivalently with $\{\boldsymbol{s}, \boldsymbol{e}\}(\mathbf{x}, t) = \mathrm{Re}\{\{\hat{\boldsymbol{s}}, \hat{\boldsymbol{e}}\}(\mathbf{x})\mathrm{e}^{-\mathrm{i}\omega t}\}$ (2.9) becomes

$$\hat{\boldsymbol{s}} = 2\hat{\mu}\hat{\boldsymbol{e}}, \quad \mathrm{tr}(\hat{\boldsymbol{\sigma}}) = 3[(K - \mathrm{i}\omega\eta_K)\mathrm{tr}(\hat{\varepsilon}) - \alpha K T_0 \hat{\theta}]. \tag{2.15}$$

Substituting (2.14) in the conservation of momentum equation (2.1b) yields

$$(\hat{\lambda} + 2\hat{\mu})\nabla(\nabla \cdot \hat{\mathbf{u}}) - \hat{\mu}\nabla \times \nabla \times \hat{\mathbf{u}} + \rho_0\omega^2\hat{\mathbf{u}} = \alpha K T_0 \nabla\hat{\theta}, \tag{2.16}$$

which corresponds to Navier–Lamé with thermo-mechanical coupling as in classical linear TE. Introducing the classical Helmholtz potentials ϕ, Φ in the form

$$\hat{\mathbf{u}} = \nabla\phi + \nabla \times \Phi, \quad \nabla \cdot \Phi = 0, \tag{2.17}$$

and making use of Helmholtz's theorem [26], we deduce that the potentials must satisfy

$$\Delta\phi + k_\phi^2\phi + L_\theta\hat{\theta} = 0, \tag{2.18a}$$

$$\Delta\Phi + k_\Phi^2\Phi = \mathbf{0} \tag{2.18b}$$

and

$$\Delta\hat{\theta} + k_\theta^2\hat{\theta} + L_\phi\Delta\phi = 0, \tag{2.18c}$$

where

$$k_\theta^2 = \mathrm{i}c_v\frac{\rho_0\omega}{\mathscr{K}}, \quad k_\phi^2 = \frac{\rho_0\omega^2}{\hat{\lambda} + 2\hat{\mu}}, \quad k_\Phi^2 = \frac{\rho_0\omega^2}{\hat{\mu}}, \tag{2.19}$$

and where we have defined L_ϕ (with dimension m^{-2}), and the non-dimensional thermo-mechanical coupling parameter L_θ as

$$L_\phi = \frac{\mathrm{i}\alpha K\omega}{\mathscr{K}} \quad \text{and} \quad L_\theta = -\frac{\alpha T_0 K}{\hat{\lambda} + 2\hat{\mu}}. \tag{2.20}$$

In the limit $\alpha \to 0$ the system (2.18) uncouples immediately. Moreover, it is the size of $|L_\theta|$ that determines the importance of thermo-elastic coupling. In order to obtain a less restrictive theory, it is often argued for many materials in common scenarios that $|L_\phi| \times$ ('characteristic length')$^2 \ll 1$ so that the energy equation (2.18c) becomes uncoupled. The corresponding solution can then be fed into (2.18a) to obtain a forced Helmholtz equation with a known source term. This approximation is sometimes referred to as the *theory of thermal stresses* in order to distinguish it from fully coupled thermo-elasticity [27].

To decouple the system (2.18) completely substitute (2.18a) into (2.18c) to obtain

$$\mathcal{L}_O\{\phi\} = 0, \quad \text{where } \mathcal{L}_O = (\Delta + (a - b))(\Delta + (a + b)) \tag{2.21}$$

$$a = \frac{1}{2}(k_\theta^2 + k_\phi^2 - L_\theta L_\phi) \quad \text{and} \quad b = \sqrt{a^2 - k_\phi^2 k_\theta^2}. \tag{2.22}$$

The solution to (2.21) is thus equivalent to solving the pair of Helmholtz equations

$$\Delta\vartheta + k_\vartheta^2\vartheta = 0 \tag{2.23a}$$

and

$$\Delta\varphi + k_\varphi^2\varphi = 0, \tag{2.23b}$$

with

$$k_\vartheta^2 = a + b \quad \text{and} \quad k_\varphi^2 = a - b. \tag{2.24}$$

Employing (2.18a), the two newly introduced potentials φ, ϑ are related to ϕ and $\hat{\theta}$ via the matrix form[2]

$$\begin{pmatrix} \phi \\ \hat{\theta} \end{pmatrix} = \begin{pmatrix} 1 & 1 \\ \mathscr{T}_\varphi & \mathscr{T}_\vartheta \end{pmatrix} \begin{pmatrix} \varphi \\ \vartheta \end{pmatrix}, \tag{2.25}$$

where

$$\mathscr{T}_\varphi = \frac{1}{L_\theta}(k_\varphi^2 - k_\phi^2) \quad \text{and} \quad \mathscr{T}_\vartheta = \frac{1}{L_\theta}(k_\vartheta^2 - k_\phi^2). \tag{2.26}$$

As is well known therefore, the equations of motion for linear local-in-time TVE are thus governed by the three Helmholtz equations (2.18b), (2.23a) and (2.23b) from which we can recover the temperature and displacement fields through (2.17), and (2.25). These wave potentials consist of two thermo-compressional potentials φ, ϑ and a shear potential Φ, the latter being independent of thermal effects. They can be directly correlated to those of [28] as well as [29] (by taking the limit of zero volume fraction of voids). Asymptotic approximations to (2.24), (2.26) and their validity will be discussed in §2d but before this we move on to incorporating the influence of stress relaxation.

Finally, as we will see later, it is useful to represent the intensity of time-harmonic waves as an average of $\mathbf{J}$ (2.12) over the wave period $(2\pi/\omega)$ such that

$$\langle \mathbf{J} \rangle(\mathbf{x}, \omega) = \frac{\omega}{2\pi} \int_0^{2\pi/\omega} \mathbf{J}(\mathbf{x}, t) \, dt = -\frac{1}{2} \operatorname{Re}\{\boldsymbol{\sigma} \dot{\mathbf{u}}^* + \theta \mathscr{K} \nabla \theta^*\}, \tag{2.27}$$

where asterisk * denotes complex conjugate. Equation (2.27) represents the average energy flux (per unit area) due to both the mechanical power and the heat flux, see e.g. [25].

(c) Non-local (in time) thermo-visco-elastic: the influence of stress relaxation

The local-in-time TVE constitutive model (2.7a) has no dependence on *history*, or equivalently as it turns out, no information with regard to stress rates. While the model as presented permits the modelling of *creep compliance*, it means that *stress relaxation* cannot be modelled. From a physical viewpoint, this limits its applicability, especially for the diverse range of polymeric materials in which relaxation, or equivalently, strongly frequency-dependent material properties, is common. In order to accommodate this effect *and* creep, we must take into consideration the kinematical and thermal *time histories*, so that the Helmholtz free energy per unit mass now takes the form

$$\Psi \equiv \Psi(\varepsilon(\tau)|_{\tau=-\infty}^t, T(\tau)|_{\tau=-\infty}^t). \tag{2.28}$$

This makes the question of whether the Clausius–Duhem inequality (2.1d) is solved less trivial, even for linear theories [30,31]. Instead, following [30] the equations for a linear isotropic medium (2.7), (2.9) generalize to

$$s = \int_{-\infty}^t \mathcal{R}_1(t - \mathcal{T})\dot{e}(\mathcal{T}) \, d\mathcal{T}, \tag{2.29a}$$

$$\operatorname{tr}(\boldsymbol{\sigma}) = \int_{-\infty}^t \mathcal{R}_2(t - \mathcal{T})\operatorname{tr}(\dot{\varepsilon}(\mathcal{T})) \, d\mathcal{T} - 3T_0 \int_{-\infty}^t \mathcal{R}_3(t - \mathcal{T})\dot{\theta}(\mathcal{T}) \, d\mathcal{T} \tag{2.29b}$$

and

$$\rho_0 \mathfrak{s} = \rho_0 \mathfrak{s}_0 + T_0 \int_{-\infty}^t \mathcal{R}_4(t - \mathcal{T})\dot{\theta}(\mathcal{T}) \, d\mathcal{T} + \int_{-\infty}^t \mathcal{R}_3(t - \mathcal{T})\operatorname{tr}(\dot{\varepsilon}(\mathcal{T})) \, d\mathcal{T}, \tag{2.29c}$$

and the energy equation (2.10) is replaced by

$$\mathscr{K}\Delta\theta = \frac{\partial}{\partial t}\left(T_0 \int_{-\infty}^t \mathcal{R}_4(t - \mathcal{T})\dot{\theta}(\mathcal{T}) \, d\mathcal{T} + \int_{-\infty}^t \mathcal{R}_3(t - \mathcal{T})\operatorname{tr}(\dot{\varepsilon}(\mathcal{T})) \, d\mathcal{T} \right), \tag{2.30}$$

---

[2]Owing to the uniqueness of the solution to the linear PDE (2.21) being up to a constant, we may also write $\phi = C_1\varphi + C_2\vartheta$, whence $\hat{\theta}L_\theta = C_1(k_\varphi^2 - k_\phi^2)\varphi + C_2(k_\vartheta^2 - k_\phi^2)\vartheta$, for constants C_1, C_2 but here we choose $C_1 = C_2 = 1$ to match the conventional approach.

where the kernels $\mathcal{R}_1, \mathcal{R}_2, \mathcal{R}_3, \mathcal{R}_4$ are relaxation functions[3] containing the time varying thermo-mechanical properties of the medium. Note that despite including thermal history in the present theory, general thermodynamic consistency again requires Fourier's Law (2.6) to hold with a constant thermal conductivity $\mathscr{K}$ [30], so that (2.30) remains parabolic.

Restrictions on $\mathcal{R}_i$ include causality, giving $\mathcal{R}_i(\tau) = 0$ for $\tau < 0$ (where $i = 1$–4) and choosing a form such that all integrals in (2.29), (2.30) are convergent. Finally, the choice must satisfy the *dissipation inequality*[4]:

$$\Lambda \geq 0, \tag{2.31}$$

where Λ is detailed in electronic supplementary material Section SM2. Despite being frequently neglected, the requirement (2.31) is also present in the analogue isothermal VE theory. For a particular choice of $\mathcal{R}_i$, it can in principle be checked whether (2.31) is satisfied. We note that the thermodynamics of certain widely used theories are often unclear, as in the case of Fung's Quasilinear visco-elasticity (QLV) theory [32]. Unless otherwise stated, in the subsequent work we assume that we meet the necessary requirements for equations (2.29)–(2.30) to apply.

In general it is non-trivial to determine the time-dependent form of the relaxation functions for a given material. They are assumed to depend only on the background temperature (assumed constant) T_0 as any more general temperature dependence must involve non-linearities, which are outside the scope of this paper. An exception is given by 'thermo-rheologically simple' materials [33], where the dependence of the material properties on temperature has a particularly appealing structure that allows for description with a linear theory. The dependence of these properties on temperature can be associated with a shift of the behaviour at a base constant temperature which is commonly known as the '*time-temperature superposition*'. The particular shift function can in general be found experimentally but a very common empirical shift function is that of the Williams-Landel-Ferry [21].

Having established a sufficiently general constitutive framework with which to model materials with time-dependent material properties we now discuss how this can be described in the frequency domain.

(i) Frequency domain decomposition for the non-local equations

Assume now that the fields are time-harmonic, of the form

$$\{\mathbf{u}, \theta, \boldsymbol{\sigma}, \mathbf{s}, \varepsilon, \boldsymbol{e}\}(\mathbf{x}, t) = \mathrm{Re}\,\{\{\hat{\mathbf{u}}, \hat{\theta}, \hat{\boldsymbol{\sigma}}, \hat{\mathbf{s}}, \hat{\varepsilon}, \hat{\boldsymbol{e}}\}(\mathbf{x}) \mathrm{e}^{-\mathrm{i}\omega t}\}, \tag{2.32}$$

and decompose all relaxation functions as

$$\mathcal{R}_i(t) = \mathcal{R}_i{}' + \mathscr{R}_i(t), \quad \text{s.t.} \ \mathscr{R}_i(t) \to 0 \quad \text{as } t \to \infty, \tag{2.33}$$

for $i = 1, 2, 3, 4$, where $\mathcal{R}_i{}'$ denotes the long-time asymptote, in the limit $t \to \infty$, and $\mathscr{R}_i(t)$ is the time-dependent part. This makes the treatment of the frequency transforms below simpler [31].

We can then substitute (2.32) with (2.33) into (2.29) to obtain

$$\hat{\mathbf{s}} = 2\tilde{\mu}(\mathrm{i}\omega)\hat{\boldsymbol{e}} \quad \text{and} \quad \mathrm{tr}(\hat{\boldsymbol{\sigma}}) = 3[\tilde{K}(\mathrm{i}\omega)\mathrm{tr}(\hat{\varepsilon}) - T_0\tilde{\mathcal{R}}_3(\mathrm{i}\omega)\hat{\theta}], \tag{2.34}$$

which may be directly compared to (2.15). In order to write (2.34), we have defined

$$\tilde{\mu}(\mathrm{i}\omega) = \frac{1}{2}\left(\mathcal{R}_1' - \mathrm{i}\omega \int_0^\infty \mathscr{R}_1(\mathcal{V})\mathrm{e}^{\mathrm{i}\omega\mathcal{V}}\,\mathrm{d}\mathcal{V}\right), \quad \tilde{K}(\mathrm{i}\omega) = \frac{1}{3}\left(\mathcal{R}_2' - \mathrm{i}\omega \int_0^\infty \mathscr{R}_2(\mathcal{V})\mathrm{e}^{\mathrm{i}\omega\mathcal{V}}\,\mathrm{d}\mathcal{V}\right) \tag{2.35a}$$

and

$$\tilde{\mathcal{R}}_3(\mathrm{i}\omega) = \mathcal{R}_3' - \mathrm{i}\omega \int_0^\infty \mathscr{R}_3(\mathcal{V})\mathrm{e}^{\mathrm{i}\omega\mathcal{V}}\,\mathrm{d}\mathcal{V}, \tag{2.35b}$$

which, respectively, corresponds to the complex shear modulus, the three-dimensional complex bulk modulus, and the complex modulus associated with the coefficient of thermo-mechanical

---

[3]Here these functions are scalar valued since we are only considering isotropic deformations.

[4]Unlike in the local case above where this inequality is automatically satisfied by setting constant valued viscosities, the generality of time non-locality implies an extra restriction on the relaxation functions.

coupling. From (2.35a), it follows that we can define the generalized first Lamé modulus, Poisson's ratio and Young's modulus, respectively, as [34]

$$\tilde{\lambda}(i\omega) = \tilde{K}(i\omega) - \frac{2}{3}\tilde{\mu}(i\omega), \quad \tilde{\nu}(i\omega) = \frac{3\tilde{K}(i\omega) - 2\tilde{\mu}(i\omega)}{6\tilde{K}(i\omega) + 2\tilde{\mu}(i\omega)}, \quad \tilde{E}(i\omega) = \frac{9\tilde{K}(i\omega)\tilde{\mu}(i\omega)}{3\tilde{K}(i\omega) + \tilde{\mu}(i\omega)}. \tag{2.36}$$

Finally, using (2.35b) the energy balance equation (2.30) becomes

$$\mathscr{K}\,\Delta\hat{\theta} + i\omega(T_0\tilde{\mathcal{R}}_4(i\omega)\hat{\theta} + \tilde{\mathcal{R}}_3(i\omega)\mathrm{tr}(\hat{\varepsilon})) = 0, \tag{2.37}$$

where we defined the complex modulus

$$\tilde{\mathcal{R}}_4(i\omega) = \mathcal{R}'_4 - i\omega\int_0^\infty \mathscr{R}_4(\mathcal{V})\mathrm{e}^{i\omega\mathcal{V}}\,\mathrm{d}\mathcal{V}. \tag{2.38}$$

In fact, by direct comparison with the energy equation commonly used in linear thermo-elasticity (e.g. (1.12.22) in [18]) we observe that this quantity can be interpreted as a specific heat at constant strain/volume per unit volume, which in the setting of TVE with temperature history allows for frequency dependency, i.e.

$$\tilde{\mathcal{R}}_4(i\omega) = \frac{\rho_0}{T_0}\tilde{c}_v(i\omega). \tag{2.39}$$

Hence, the associated Cauchy stress in the frequency domain becomes

$$\hat{\boldsymbol{\sigma}}^{\mathrm{TVE}} = 2\tilde{\mu}(i\omega)\hat{\boldsymbol{e}} + (\tilde{K}(i\omega)\mathrm{tr}(\hat{\varepsilon}) - T_0\tilde{\mathcal{R}}_3(i\omega)\hat{\theta})\boldsymbol{I} = 2\tilde{\mu}(i\omega)\hat{\varepsilon} + (\tilde{\lambda}(i\omega)\mathrm{tr}(\hat{\varepsilon}) - T_0\tilde{\mathcal{R}}_3(i\omega)\hat{\theta})\boldsymbol{I}. \tag{2.40}$$

The associated energy and momentum equations reduce to

$$\mathscr{K}\,\Delta\hat{\theta} + i\omega\rho_0\tilde{c}_v(i\omega)\hat{\theta} + i\omega\tilde{\mathcal{R}}_3(i\omega)\boldsymbol{\nabla}\cdot\hat{\mathbf{u}} = 0 \tag{2.41a}$$

and

$$(\tilde{\lambda}(i\omega) + 2\tilde{\mu}(i\omega))\boldsymbol{\nabla}(\boldsymbol{\nabla}\cdot\hat{\mathbf{u}}) - \tilde{\mu}(i\omega)\boldsymbol{\nabla}\times\boldsymbol{\nabla}\times\hat{\mathbf{u}} - T_0\tilde{\mathcal{R}}_3(i\omega)\nabla\hat{\theta} + \rho_0\omega^2\hat{\mathbf{u}} = \mathbf{0}. \tag{2.41b}$$

Conveniently, equations (2.40)–(2.41b) have the same structure as (2.13)–(2.16), (2.18), for a fixed frequency ω. Now however, rich frequency-dependent behaviour can be accommodated by the incorporation of the relaxation functions. The equivalent form means that the decomposition of §2b(i) remains valid so that the fields remain solutions of the decoupled Helmholtz equations (2.18b), (2.23a) and (2.23b), as in the local case, with the only change (but a critical one) being that now the relevant quantities appearing in the wavenumbers have a more general frequency dependence:

$$k_\theta^2 = i\tilde{c}_v(i\omega)\frac{\rho_0\omega}{\mathscr{K}}, \quad k_\phi^2 = \frac{\rho_0\omega^2}{\tilde{\lambda}(i\omega) + 2\tilde{\mu}(i\omega)}, \quad k_\Phi^2 = \frac{\rho_0\omega^2}{\tilde{\mu}(i\omega)} \tag{2.42a}$$

and

$$L_\phi = \frac{i\omega\tilde{\mathcal{R}}_3(i\omega)}{\mathscr{K}}, \quad L_\theta = -\frac{T_0\tilde{\mathcal{R}}_3(i\omega)}{\tilde{\lambda}(i\omega) + 2\tilde{\mu}(i\omega)}. \tag{2.42b}$$

As in the local case, the displacement and temperatures are given, respectively, by appropriate combinations of the potentials:

$$\hat{\mathbf{u}}^{\mathrm{TVE}} = \nabla(\vartheta + \varphi) + \nabla\times\boldsymbol{\Phi} \tag{2.43a}$$

and

$$\hat{\theta}^{\mathrm{TVE}} = \frac{1}{L_\theta}(a - b - k_\phi^2)\varphi + \frac{1}{L_\theta}(a + b - k_\phi^2)\vartheta. \tag{2.43b}$$

Note, in particular, that the more general frequency dependence of the TVE coupling parameter L_θ shows that certain materials may exhibit significant thermal coupling only for certain frequency ranges.
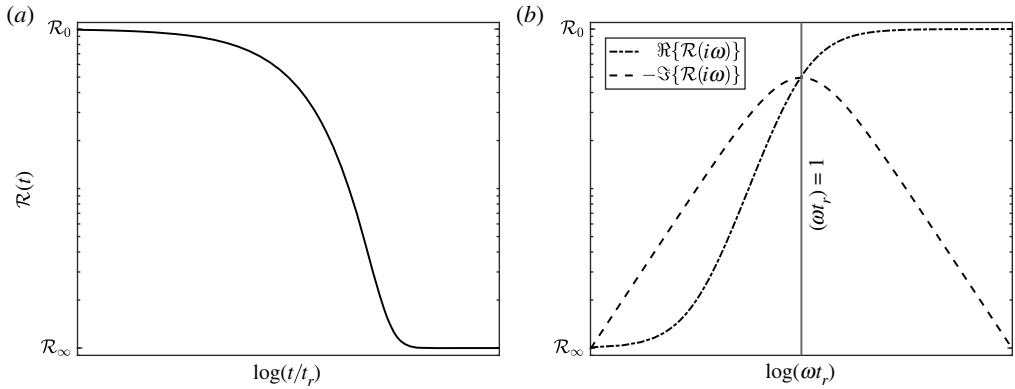
Figure 1. An example of prototype, single relaxation time, scalar relaxation function time-domain behaviour (a) given by (2.45), and its frequency domain counterpart (b) from (2.46).

(ii) Form of relaxation functions

Stress relaxation tests aim to investigate the viscoelastic properties of a given sample of material via specific loading modes, e.g. shear, uniaxial or bi-axial compression, etc. A general expression for relaxation functions is the so-called *Prony series* [16], which takes the form

$$\mathcal{R}(t) = \left(\mathcal{R}_\infty + \sum_{n=1}^{N} \mathcal{R}_n \, e^{-t/t_n} \right) H(t), \tag{2.44}$$

where $H(\circ)$ denotes the Heaviside function and t_n are characteristic relaxation times of the medium in question. $\mathcal{R}_\infty$ is the associated *long-term modulus*, resulting from the limit $t \to \infty$, while $\mathcal{R}_0 = \mathcal{R}_\infty + \sum_{n=1}^{N} \mathcal{R}_n$ is the *instantaneous* modulus. In practice, modes of deformation or propagation are chosen that can isolate the dependence of relaxation functions so that they can be measured experimentally [35]. A common scenario for the purposes of modelling is to assume a single relaxation time ($t_1 = t_r$), which is often referred to as the *Standard linear solid model* (SLSM):

$$\mathcal{R}(t) = (\mathcal{R}_\infty + (\mathcal{R}_0 - \mathcal{R}_\infty)e^{-t/t_r})H(t), \tag{2.45}$$

where in practice the relaxation time is obtained by fitting the model to the relaxation test data [16]. Following (2.35), (2.38), in the frequency domain (2.45) becomes

$$\mathcal{R}(i\omega) = \mathcal{R}_\infty - (\mathcal{R}_0 - \mathcal{R}_\infty)\frac{i\omega t_r}{1 - i\omega t_r}, \tag{2.46}$$

and it is apparent from (2.46) that, in the low-frequency (long time, or *rubbery*) and high-frequency (short time, or *glassy*) limits, $\mathcal{R}_\infty$ and $\mathcal{R}_0$ are, respectively, obtained (figure 1). When separating (2.46) into real and imaginary parts, the 'loss tangent' may be defined which is frequently used in order to characterize viscoelastic losses under steady-state oscillatory conditions and associated experimental data [36]. In practice, the ratio $\mathcal{R}_0/\mathcal{R}_\infty$ can be very large, up to several orders of magnitude, see e.g. [4] for the shear modulus of an unfilled cross-linked rubber material.

Temperature can play a very important role in the behaviour of the moduli [1,3]. Linear TVE theory allows only for dependence of the mechanical properties on the background temperature T_0 as is the case in an isothermal theory. Stress relaxation tests as described above are associated with specific modes of deformation and, therefore, the corresponding data obtained provides, e.g. the time-dependent Young's modulus (e.g. $\mathcal{R}(t)$ in (2.45)) under uniaxial compression or tension. On the other hand, several other experimental methods are used to approximate the shear modulus, e.g. [3]. As a result, one would expect that for an isotropic medium these two independent constants are sufficient to describe the continuum in consideration. It turns

out that this is often not the case due to the required accuracy of the experiments, and tests involving primarily volumetric effects are necessary [34]. This is particularly evidenced for nearly incompressible elastic materials, and a method to determine $\tilde{K}(i\omega)$ was presented in [37], where it is assumed that bulk loss is a constant fraction of the loss in shear. This assumption led to good agreement with the observed experimental results, for polyethylene (PE) and Plexiglass (PMMA) the bulk loss ($\mathrm{Im}\{\tilde{K}\}/\mathrm{Re}\{\tilde{K}\}$) represents 20% of the shear loss, whereas in polystyrene the bulk loss was calculated to be around 0.1%. Nevertheless, to this day, data for bulk losses in general materials remains difficult to find, as discussed in [38].

The frequency dependence of the specific heat and thermo-mechanical coupling term in (2.35b) and (2.38) are reported even less, and these quantities are usually considered static, although relaxation-type phenomena of the specific heat has been observed, e.g. [39]. This discussion for VE behaviour together with the thermal properties illustrates the intricacies involved in the correct determination of many of the quantities appearing in a TVE model. As a result, in studies seeking more qualitative results over a wider range of materials, common simplifications are made. In [40], it is argued that in most instances VE effects are mainly related to the isochoric part of the deformation and therefore if we write the Cauchy stress (2.40) in terms of the hydrostatic and deviatoric parts we have (recalling (2.8))

$$\hat{\boldsymbol{\sigma}} = 2\tilde{\mu}(i\omega)\hat{\boldsymbol{e}} + (K\mathrm{tr}(\varepsilon) - T_0\tilde{\mathcal{R}}_3(i\omega)\hat{\theta})\boldsymbol{I}, \tag{2.47}$$

where K becomes a real valued constant from which the value of $\tilde{\lambda}(i\omega)$ follows through (2.36). In [2] it is instead assumed that Young's modulus takes the form (2.46), while Poisson's ratio is kept constant. In turn, this implies that the shear modulus also takes the form (2.46). The magnitude of the variation in the specific heat is such that it will be assumed constant.

(iii) Relaxation function interpretation of local thermo-visco-elastic

The local TVE model discussed in §2b can be thought of as a special case from that of §2c where the kinematical and thermal time histories represented by $\mathcal{R}_1, \mathcal{R}_2, \mathcal{R}_3, \mathcal{R}_4$ in (2.29) are described by Heaviside and delta functions. In the frequency domain, this simply results in the choice

$$\tilde{\lambda}(i\omega) = \lambda - i\omega\eta_\lambda, \quad \tilde{\mu}(i\omega) = \mu - i\omega\eta_\mu, \quad \tilde{c}_v(i\omega) = c_v, \quad \tilde{\mathcal{R}}_3(i\omega) = \alpha K, \tag{2.48}$$

in (2.40)–(2.41b) to arrive at the local TVE theory. In the time domain, the instantaneous local viscous effects are represented by delta functions (e.g. [24]) such that for the shear modulus

$$\mathcal{R}_1(t) = 2(\mu H(t) + \eta_\mu \delta(t)). \tag{2.49}$$

This can be deduced by taking the inverse Fourier transform of $(2.35a)_1$, and similarly for the bulk modulus. The time domain representation for the shear modulus (2.49) shows how relaxation effects as discussed in §2c(ii) are clearly not captured with local TVE. In the frequency domain, the real part remains constant, whereas the imaginary part becomes unbounded as the frequency increases. For this reason, local TVE is in general not suitable in studies beyond single frequency analyses. Given that in general we are interested in wave propagation in materials over rather general frequencies this is significantly restrictive.

Next we consider asymptotic limits under which thermo-compressional coupling can be significantly simplified in the context of the general TVE theory, before moving onto specific physical limits in the next section.

(d) Asymptotic approximations for thermo-compressional coupling

Here we simplify the thermo-compressional wavenumbers $a \pm b = a \pm \sqrt{a^2 - k_\phi^2 k_\theta^2}$ in (2.24), and the temperature field (2.43b) by identifying one small parameter. We note that, different to several references stemming from [41] for fluids, we find we only need one small parameter, rather than

two, to reach a simple and accurate model. Asymptotic analysis illustrates that k_φ is a quasi-mechanical wavenumber, while k_ϑ is a quasi-thermal wavenumber. Similar expressions for one-dimensional TVE waves are given in [31], section 6.3.

For a vast range of frequencies and materials, including solids, liquids and gases, it can be observed that the pressure dominated wavelength is far longer than the thermal-dominated wavelength, which leads us to the small parameter[5]:

$$|\delta| \ll 1 \quad \text{where} \quad \delta = \frac{k_\phi^2}{k_\theta^2} = \frac{-i\omega \mathcal{K}}{c_v(i\omega)(\tilde{\lambda}(i\omega) + 2\tilde{\mu}(i\omega))}, \tag{2.50}$$

and we further assume that

$$|\delta| \ll \left| \frac{L_\phi L_\theta}{k_\theta^2} \right|. \tag{2.51}$$

The right side of the inequality (2.51) is a non-dimensional number related to the coupling between thermal and pressure modes. If the right side of (2.51) is of the same order as δ, or smaller, then the structure of the asymptotics below changes, as there will be almost no coupling between thermal and pressure modes. To summarize, inequality (2.51) is a necessary condition for these modes to be coupled. The inequality (2.51) is also equivalent to $\omega \mathcal{K} \ll c_v K(\gamma - 1)$ which for a given material can be a useful upper bound on the admissible frequency of the expansions below. Based on the discussion in §2c(ii), we will neglect thermal histories and thus write $\tilde{c}_v(i\omega) = c_v$, $\tilde{\mathcal{R}}_3(i\omega) = \alpha K$. Expanding in δ then,

$$b = \pm \frac{1}{2} \left[k_\theta^2 - L_\theta L_\phi - \frac{k_\theta^4 + k_\theta^2 L_\theta L_\phi}{k_\theta^2 - L_\theta L_\phi} \delta - \frac{2k_\theta^6 L_\theta L_\phi}{(k_\theta^2 - L_\theta L_\phi)^3} \delta^2 + O(\delta^3) \right],$$

where the sign chosen depends on the complex argument of the term within the square-root, and the chosen branch cut. Depending on this choice, we will have either $a \pm b = k_\varphi^2$ and $a \mp b = k_\vartheta^2$, with k_φ^2 and k_ϑ^2 shown below:

$$k_\varphi^2 = \frac{k_\theta^4}{k_\theta^2 - L_\theta L_\phi} \delta + \frac{k_\theta^6 L_\theta L_\phi}{(k_\theta^2 - L_\theta L_\phi)^3} \delta^2 + O(\delta^3) \tag{2.52a}$$

and

$$k_\vartheta^2 = k_\theta^2 - L_\theta L_\phi - \frac{k_\theta^2 L_\theta L_\phi}{k_\theta^2 - L_\theta L_\phi} \delta + O(\delta^2). \tag{2.52b}$$

Similarly, we can now expand the temperature contributions $(a \pm b - k_\phi^2)/L_\theta$ given in (2.26). We find

$$\mathcal{T}_\varphi = \frac{1}{L_\theta}(k_\varphi^2 - k_\phi^2) = \frac{k_\theta^2 L_\phi}{k_\theta^2 - L_\theta L_\phi} \delta + \frac{k_\theta^6 L_\phi}{(k_\theta^2 - L_\theta L_\phi)^3} \delta^2 + O(\delta^3) \tag{2.53a}$$

and

$$\mathcal{T}_\vartheta = \frac{1}{L_\theta}(k_\vartheta^2 - k_\phi^2) = \frac{k_\theta^2 - L_\theta L_\phi}{L_\theta} - \frac{k_\theta^4}{k_\theta^2 - L_\theta L_\phi} \delta + O(\delta^2), \tag{2.53b}$$

so that $\mathcal{T}_\varphi(\mathcal{T}_\vartheta)$ is the temperature contribution corresponding to the mode with wavenumber $k_\varphi(k_\vartheta)$. An illustration of the accuracy of the expansions for the thermo-compressional wavenumbers for different materials is given in figure 2. Similar results were obtained for the temperature contributions (2.53) but have not been included here.

3. Limits to theories that neglect specific physical effects

A plethora of approximate thermo-visco-elastic theories exist that neglect certain physical effects. Here we describe such theories in terms of parameter limits of the general TVE theory described above, noting that we have already described how local TVE is recovered from non-local TVE

---

[5]Alternatively, we could just have assumed that $|a^2| \ll |k_\phi^2 k_\theta^2|$, but this approach is avoided since its physical interpretation is not straightforward.
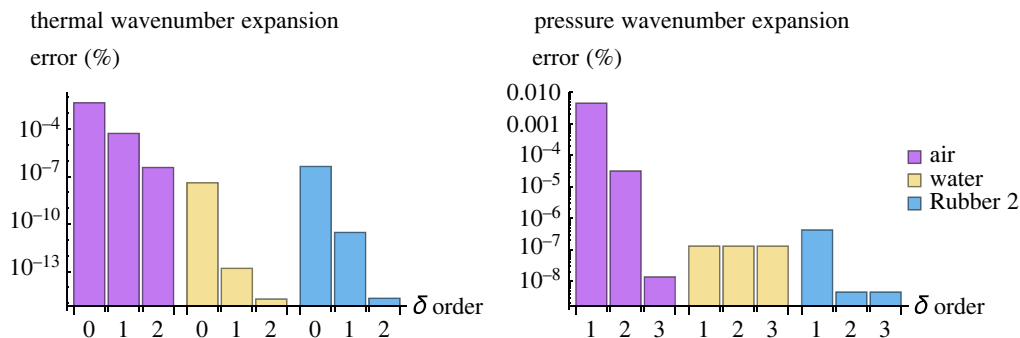
Figure 2. Maximum relative errors for the asymptotic expansions (2.52) for a frequency range of 10 kHz to 10 MHz and material parameters from table 4. For Rubber 2, the shear modulus is described by the single Prony term relaxation function (2.46) where the frequencies cover both the rubber and glassy phase. (Online version in colour.)
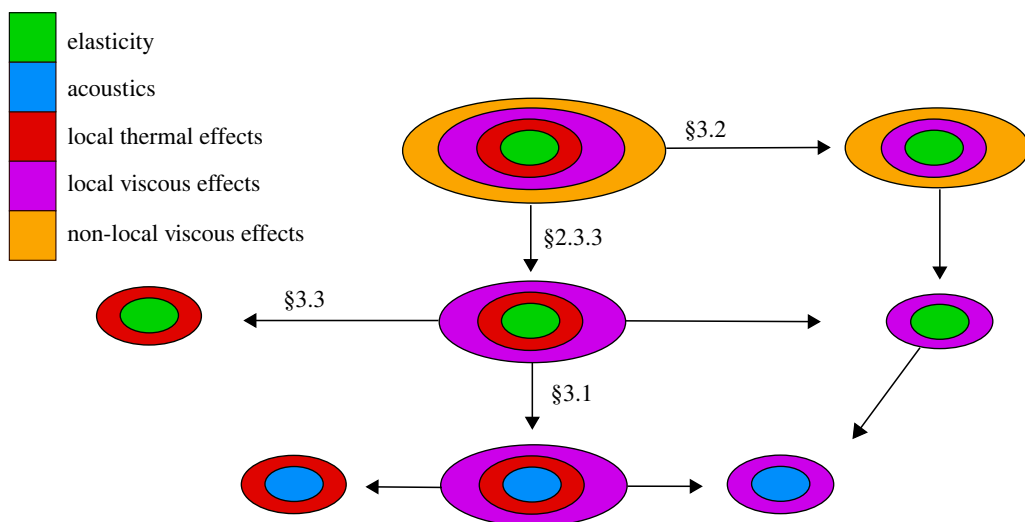
Figure 3. Representation of various elasto/acoustic dissipative theories, where the arrows indicate various limits that can be taken to arrive at other (more restrictive) theories. (Online version in colour.)

in §2c(iii) via the choice of specific relaxation functional forms. More generally, it is important to understand how significant the neglected terms are when the full TVE is compared with the simpler theories. The efficacy of the various limits is thus studied with regard to a canonical problems involved half-spaces in §4.

Figure 3 summarizes the various limits taken from the TVE theory in the frequency domain, starting from the current general framework, where various effects can be switched off and on to yield various commonly used theories. Other relevant dissipative theories concerning thermal relaxation in solids and those involving molecular relaxation effects in the acoustics of gases are not included since these require further modelling considerations, (see e.g. Section 2.4 in [7]).

(a) Thermo-visco-acoustic fluids

Starting with the local TVE theory described in §2b and taking the standard limit of zero shear modulus

$$\mu \to 0, \tag{3.1}$$

leads to the widely used model for (local in time) thermo-visco-acoustics [7,42]. In this regime, the thermodynamic identity (2.11) becomes

$$\gamma - 1 = \frac{\alpha^2 T_0 c_{\text{Iso}}^2}{c_v}, \quad \text{where } c_{\text{Iso}}^2 = \frac{\lambda_{\text{Iso}}}{\rho_0}, \tag{3.2}$$

since in the limit $K_{\text{Iso}} \to \lambda_{\text{Iso}}$. The subscript 'Iso' in the definition of the isothermal sound speed c_{Iso} is chosen to emphasize that these quantities are defined at a state of constant temperature[6] (see e.g. (78) in [38]). Note that here the Lamé parameters are isothermal by definition ($\lambda \equiv \lambda_{\text{Iso}}$) since the Helmholtz free energy is expanded from a state of constant temperature T_0 and zero strain (see (A 1) in appendix A). With (3.1) the thermo-mechanical coupling constant L_θ (2.20) can be approximated by $L_\theta \approx -\alpha T_0$ since for frequencies of interest we have $\omega\eta_\lambda, \omega\eta_\mu \ll \lambda$. Furthermore, with (3.1) and (3.2) the quantities (2.19) and (2.20) become

$$k_\theta^2 = \frac{i\rho_0\omega c_p}{\gamma\mathscr{K}}, \quad k_\phi^2 \to \frac{\rho_0\omega^2}{\rho_0 c_{\text{Iso}}^2 - i\omega\zeta}, \quad k_\Phi^2 \to \frac{i\rho_0\omega}{\eta_\mu} \tag{3.3a}$$

and

$$L_\phi \to \frac{i\rho_0\omega\alpha c_{\text{Iso}}^2}{\mathscr{K}}, \qquad L_\theta \to -\frac{\alpha\rho_0 c_{\text{Iso}}^2 T_0}{\rho_0 c_{\text{Iso}}^2 - i\omega\zeta}, \tag{3.3b}$$

with $\zeta = \eta_\lambda + 2\eta_\mu$ and given that $c_v = c_p/\gamma$. With (3.3) and in the limit $\mu \to 0$, the linear operator (2.21) becomes

$$\mathcal{L}_O \to \mathcal{L}_{\text{TVA}} = (\rho_0 c_A^2 - i\omega\zeta\gamma)\mathscr{K}\nabla^4 + i\omega[\rho_0^2 c_A^2 c_p - i\omega\rho_0(c_p\zeta + \mathscr{K}\gamma)]\nabla^2 + i\rho_0^2 c_p\omega^3, \tag{3.4}$$

where we have made use of (3.2) in terms of the *adiabatic* speed of sound c_A as is common in acoustics with the relation $c_A^2 = \gamma c_{\text{Iso}}^2$. The operator (3.4) is identical to that in (2.70) of [7] for TVA when the latter is written in the frequency domain and in the absence of any sources, which confirms that local TVE theory recovers TVA. Since the decomposition is unique up to a constant (as seen in (2.25)), in electronic supplementary material, section SM3, we explicitly match the current TVE potentials to those corresponding to TVA in [5].

(b) Non-local (in time) visco-elasticity

Starting with the general non-local TVE theory described above and taking the limit of zero thermo-mechanical coupling,[7] that is

$$\tilde{\mathcal{R}}_3(i\omega) \to 0, \tag{3.5}$$

in (2.40), (2.41), results in $\hat{\sigma}^{\text{VE}} = 2\tilde{\mu}(i\omega)\hat{\varepsilon} + \tilde{\lambda}(i\omega)\text{tr}(\hat{\varepsilon})\boldsymbol{I}$, as well as

$$\left(\Delta + \frac{i\omega\rho_0\tilde{c}_v(i\omega)}{\mathscr{K}}\right)\hat{\theta}^{\text{VE}} = 0 \tag{3.6a}$$

and

$$(\tilde{\lambda}(i\omega) + 2\tilde{\mu}(i\omega))\boldsymbol{\nabla}(\boldsymbol{\nabla} \cdot \hat{\mathbf{u}}) - \tilde{\mu}(i\omega)\boldsymbol{\nabla} \times \boldsymbol{\nabla} \times \hat{\mathbf{u}} + \rho_0\omega^2\hat{\mathbf{u}} = \mathbf{0}. \tag{3.6b}$$

These are the governing equations for visco-elasticity, including stress relaxation. It is apparent in (3.6) that there is no longer coupling between kinematic and thermal effects, and hence the wave

---

[6]This distinction is often ignored for liquids and solids since it is not as important (see e.g. §1.9.2 of [42]), but is paramount for gases.

[7]In the local TVE case, we simply take the limit of zero thermal expansion coefficient, that is $\alpha T_0 \to 0$.

potentials directly give

$$\hat{\mathbf{u}}^{\mathrm{VE}} = \nabla\phi + \nabla \times \boldsymbol{\Phi}, \tag{3.7}$$

where

$$\left(\Delta + \frac{\rho_0\omega^2}{\tilde{\lambda}(\mathrm{i}\omega) + 2\tilde{\mu}(\mathrm{i}\omega)}\right)\phi = 0 \quad \text{and} \quad \left(\Delta + \frac{\rho_0\omega^2}{\tilde{\mu}(\mathrm{i}\omega)}\right)\boldsymbol{\Phi} = \mathbf{0}, \tag{3.8}$$

recalling that the Lamé parameters in (3.8) are isothermal.[8] Nevertheless, in practice it is important to understand the effect of this limit on the decomposition that leads to the corresponding TVE wave potentials. It is clear that the shear wave potential remains unchanged in the limit (since it is independent of thermal effects). The situation for the thermo-compressional fields is slightly more subtle. Direct substitution of (3.5) into (2.18b), (2.23a) and (2.23b) with (2.42) leads to

$$\varphi \to C_1\phi, \quad \vartheta \to C_2\theta^{\mathrm{VE}}, \quad \text{since } a - b \to \frac{\rho_0\omega^2}{\tilde{\lambda}(\mathrm{i}\omega) + 2\tilde{\mu}(\mathrm{i}\omega)} = k_\phi^2, \ a + b \to \frac{\mathrm{i}\omega\rho_0\tilde{c}_v(\mathrm{i}\omega)}{\mathscr{K}} = k_\theta^2, \tag{3.9}$$

for some constants C_1, C_2 arising due to the uniqueness of the linear PDE solution being up to a constant. However, direct comparison between the curl free components of the TVE and VE displacements (2.43a), (3.7) implies $C_1 = 1$ and $\vartheta \to 0$ which restricts the form of C_2 but this is not sufficient to determine it explicitly. Therefore, in order to find this constant we consider the effect of the limit (3.5) on the TVE temperature (2.43b). We obtain $\mathscr{T}_\varphi \to 0$, which gives $\theta^{\mathrm{TVE}} \to (k_\theta^2 - k_\phi^2)C_2\theta^{\mathrm{VE}}/L_\theta$ (after using the second equation of (3.9)) so that in order to recover the VE solution we must choose

$$C_2 = \frac{L_\theta}{k_\theta^2 - k_\phi^2} = \frac{\mathrm{i}T_0\tilde{\mathcal{R}}_3(\mathrm{i}\omega)\mathscr{K}}{\rho_0\omega(c_v(\mathrm{i}\omega)(\tilde{\lambda}(\mathrm{i}\omega) + 2\tilde{\mu}(\mathrm{i}\omega)) + \mathrm{i}\omega\mathscr{K}}, \tag{3.10}$$

from which it is clear that in the limit both $\theta^{\mathrm{TVE}} \to \theta^{\mathrm{VE}}$ and $\vartheta \to 0$ as required. Furthermore, (local) visco–acoustic Newtonian fluids (e.g. [44]) can also be described by (3.6)–(3.8) by further letting $\mu \to 0$ so that $\mu(\omega) = -\mathrm{i}\omega\eta_\mu$ which is a convenient way to model viscous fluids like water [45,46].

(c) Thermo-elasticity

The final simplified theory is the case when viscous dissipation is neglected, leading to the theory of linear thermo-elasticity. In the frequency domain, this can be thought of as the local TVE model presented in §2b with real-valued Lamé parameters. Indeed let

$$\tilde{\lambda}(\mathrm{i}\omega) = \lambda, \quad \tilde{\mu}(\mathrm{i}\omega) = \mu, \ \tilde{c}_v(\mathrm{i}\omega) = c_v, \ \tilde{\mathcal{R}}_3(\mathrm{i}\omega) = \alpha K, \tag{3.11}$$

and substitute (3.11) in (2.40) and (2.41) so that we obtain the Cauchy stress $\hat{\boldsymbol{\sigma}}^{\mathrm{TE}} = 2\mu\hat{\varepsilon} + (\lambda\mathrm{tr}(\hat{\varepsilon}) - \alpha K T_0\hat{\theta})\boldsymbol{I}$, and the corresponding equations for time-harmonic thermo-elasticity [18]

$$\mathscr{K}\Delta\hat{\theta} + \mathrm{i}\omega\rho_0 c_v\hat{\theta} + \mathrm{i}\omega\alpha K\boldsymbol{\nabla} \cdot \hat{\mathbf{u}} = 0 \tag{3.12a}$$

and

$$(\lambda + 2\mu)\boldsymbol{\nabla}(\boldsymbol{\nabla} \cdot \hat{\mathbf{u}}) - \mu\boldsymbol{\nabla} \times \boldsymbol{\nabla} \times \hat{\mathbf{u}} - \alpha K T_0\nabla\hat{\theta} + \rho_0\omega^2\hat{\mathbf{u}} = \mathbf{0}. \tag{3.12b}$$

The structure of (3.12a), (3.12b) allows for the same decomposition $\hat{\mathbf{u}}^{\mathrm{TE}} = \nabla(\vartheta + \varphi) + \nabla \times \boldsymbol{\Phi}$, where the wave potentials must still satisfy (2.18b), (2.23a) and (2.23b) with simplified TVE parameters in (2.19), (2.20) becoming real-valued and frequency independent, i.e.

$$k_\phi^2 = \frac{\rho_0\omega^2}{\lambda + 2\mu}, \quad k_\Phi^2 = \frac{\rho_0\omega^2}{\mu}, \ L_\theta = -\frac{T_0\alpha K}{\lambda + 2\mu}, \tag{3.13}$$

whereas k_θ^2, L_φ remain unchanged.

---

[8]For the particular relations with the corresponding adiabatic moduli, see e.g. [43].
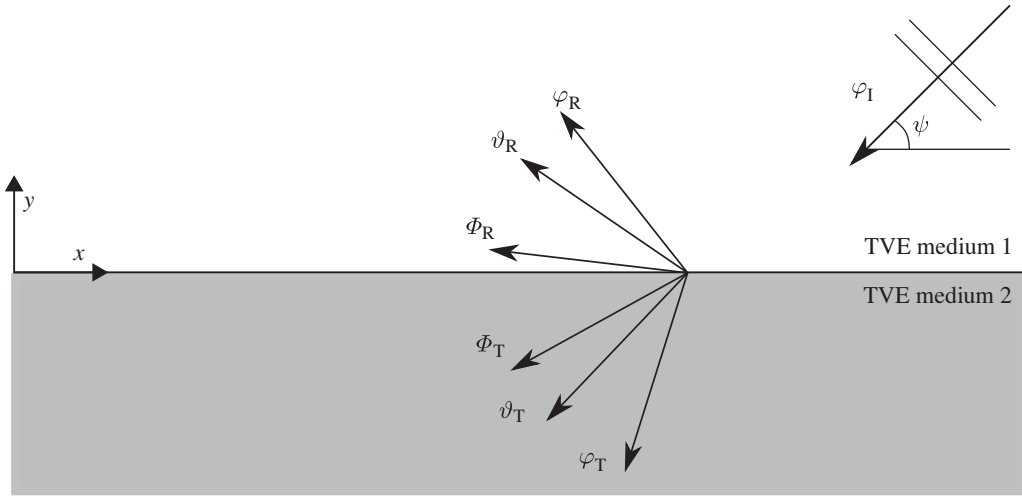
Figure 4. Schematic of the configuration of the problem of two welded semi-infinite TVE media. An incident P-dominated bulk mode impinging on the interface of the two distinct TVE domains gives rise to three reflected modes and three transmitted modes.

4. Two thermo-visco-elastic half spaces in perfect contact

To put our framework into practice, we next consider a forced boundary value problem consisting of two TVE half-spaces. In the absence of thermal effects (using the theory presented in §3b), a detailed analysis for this problem is given in [24], who generalized the work pioneered by Becker *et al*. [47] to include attenuation in reflection/transmission problems for ultrasonics. More recent work has included the presence of voids [48] or thermal relaxation [49], but only for a single traction free half-space, presumably because their goal was to understand loss mechanisms for solids.

Here we are interested in interactions between different TVE media when in contact and in particular those that are deemed as 'fluid' and 'solid'. With two half spaces, we can illustrate the advantages of the general TVE model, the limits discussed in §3, as well as the importance of stress relaxation effects (non-local in time) presented in §2c as opposed to the local TVE version in §2b, which is a common 'go to' theory when experiments are performed at specific frequencies.

(a) Problem formulation

We consider a plane-strain problem consisting of two distinct TVE half spaces in perfect contact at an interface along $y = 0$, see figure 4. All of the quantities have been non-dimensionalized following appendix (a), and relevant dimensional parameters are distinguished by an overbar.

We choose the forcing to be a pressure-dominated plane wave

$$\varphi_I = e^{-ik_{\varphi_1}(x \cos \psi + y \sin \psi)}, \quad \psi \in (0, \pi), \tag{4.1}$$

where ψ is the angle of incidence (measured anticlockwise from $y = 0$), and we assume $\mathrm{Re}\, k_{\varphi_1} \geq 0$ and $\mathrm{Im}\, k_{\varphi_1} \geq 0$. This incoming energy will be converted into reflected/transmitted thermo-compressional and shear modes. Given the translational invariance of the problem in the x-direction, each potential will depend on x through $e^{-ik_{\varphi_1} x \cos \psi}$, and therefore we write

$$\varphi_R = R_\varphi e^{ik_{\varphi_1} \sin \psi y} e^{-ik_{\varphi_1} x \cos \psi}, \quad \varphi_T = T_\varphi e^{-id_{\varphi_T} y} e^{-ik_{\varphi_1} x \cos \psi}, \tag{4.2a}$$

$$\vartheta_R = R_\vartheta e^{id_{\vartheta_R} y} e^{-ik_{\varphi_1} x \cos \psi}, \quad \vartheta_T = T_\vartheta e^{-id_{\vartheta_T} y} e^{-ik_{\varphi_1} x \cos \psi} \tag{4.2b}$$

and

$$\Phi_R = \mathbf{e}_z R_\Phi e^{id_{\Phi_R} y} e^{-ik_{\varphi_1} x \cos \psi}, \quad \Phi_T = \mathbf{e}_z T_\Phi e^{-id_{\Phi_T} y} e^{-ik_{\varphi_1} x \cos \psi}, \tag{4.2c}$$

where the potentials φ_R, ϑ_R and Φ_R are defined in the upper half space $y \geq 0$, while the potentials φ_T, ϑ_T and Φ_T are defined in the lower half space $y \leq 0$. We use subscripts R/T to denote reflected/transmitted, respectively. In the above we introduced the notation

$$
\left.\begin{aligned}
d_{\varphi_T} &= \mathrm{i}\sqrt{-(k_{\varphi_2}^2 - k_{\varphi_1}^2 \cos^2 \psi)}, \quad d_{\vartheta_R} = \mathrm{i}\sqrt{-(k_{\vartheta_1}^2 - k_{\varphi_1}^2 \cos^2 \psi)}, \\
d_{\vartheta_T} &= \mathrm{i}\sqrt{-(k_{\vartheta_2}^2 - k_{\varphi_1}^2 \cos^2 \psi)} \\
d_{\Phi_R} &= \mathrm{i}\sqrt{-(k_{\Phi_1}^2 - k_{\varphi_1}^2 \cos^2 \psi)}, \quad d_{\Phi_T} = \mathrm{i}\sqrt{-(k_{\Phi_2}^2 - k_{\varphi_1}^2 \cos^2 \psi)}.
\end{aligned}\right\}
\tag{4.3}
$$

With (4.3), when using the standard branch cut for the square root along the negative real line we have

$$
\operatorname{Im} d_{\varphi_T}, \operatorname{Im} d_{\vartheta_R}, \operatorname{Im} d_{\vartheta_T}, \operatorname{Im} d_{\Phi_R}, \operatorname{Im} d_{\Phi_T} \geq 0,
\tag{4.4}
$$

which guarantees that each of the potentials in (4.2) are bounded within their respective half spaces. In order to completely determine the potentials (4.2) we use the boundary conditions representing continuity of traction,[9] displacement, temperature and temperature flux

$$
\hat{\boldsymbol{\sigma}}_1 \mathbf{e}_y = \hat{\boldsymbol{\sigma}}_2 \mathbf{e}_y, \quad \hat{\mathbf{u}}_1 = \hat{\mathbf{u}}_2
\tag{4.5a}
$$

and

$$
\hat{\theta}_1 = \hat{\theta}_2, \quad \mathcal{K}_1 \nabla \hat{\theta}_1 \cdot \mathbf{e}_y = \mathcal{K}_2 \nabla \hat{\theta}_2 \cdot \mathbf{e}_y,
\tag{4.5b}
$$

across $y = 0$, where $\hat{\boldsymbol{\sigma}}_1$ and $\hat{\boldsymbol{\sigma}}_2$ are the stress tensors in the upper (1) and lower (2) media, respectively, while $\mathbf{u}_1$ and $\mathbf{u}_2$ are the displacements in media 1 and 2.

Substituting (4.2) into (4.5), using (2.40) and (2.43), leads to the following six equations:

$$
\begin{pmatrix}
a_{11} & a_{12} & a_{13} & a_{14} & a_{15} & a_{16} \\
a_{21} & a_{22} & a_{23} & a_{24} & a_{25} & a_{26} \\
a_{31} & a_{32} & a_{33} & a_{34} & a_{35} & a_{36} \\
a_{41} & a_{42} & a_{43} & a_{44} & a_{45} & a_{46} \\
a_{51} & a_{52} & a_{53} & a_{54} & 0 & 0 \\
a_{61} & a_{62} & a_{63} & a_{64} & 0 & 0
\end{pmatrix}
\begin{pmatrix}
R_\varphi \\ T_\varphi \\ R_\vartheta \\ T_\vartheta \\ R_\Phi \\ T_\Phi
\end{pmatrix}
=
\begin{pmatrix}
a_{11} \\ -a_{21} \\ -a_{31} \\ a_{41} \\ -a_{51} \\ a_{61}
\end{pmatrix}.
\tag{4.6}
$$

To calculate the entries a_{ij}, we provide a Mathematica notebook as supplementary material [50]. The above can be used to uniquely determine the six amplitudes $R_\varphi, T_\varphi, R_\vartheta, T_\vartheta, R_\Phi$ and T_Φ.

(b) The VE–VE limit

In the limit of no thermal coupling, we let $\alpha_1, \alpha_2 \to 0$ (and hence $k_{\varphi_1} \to k_{\phi_1}$, $k_{\varphi_2} \to k_{\phi_2}$ and $\mathcal{T}_{\varphi_1}$, $\mathcal{T}_{\varphi_2} \to 0$) in (4.6) as discussed in §3b. From this, we conclude that $R_\vartheta, T_\vartheta \to 0$ and the scattering system reduces to

$$
\begin{pmatrix}
a_{11} & a_{12} & a_{15} & a_{16} \\
a_{21} & a_{22} & a_{25} & a_{26} \\
a_{31} & a_{32} & a_{35} & a_{36} \\
a_{41} & a_{42} & a_{45} & a_{46}
\end{pmatrix}
\begin{pmatrix}
R_\varphi \\ T_\varphi \\ R_\Phi \\ T_\Phi
\end{pmatrix}
=
\begin{pmatrix}
a_{11} \\ -a_{21} \\ -a_{31} \\ a_{41}
\end{pmatrix},
\tag{4.7}
$$

where the limit of $\alpha_1, \alpha_2 \to 0$ should be taken for each of the a_{ij}. For normal incidence, $\psi = \pi/2$ we obtain the classical solutions

$$
R_\varphi = \frac{-k_{\phi_1}(\tilde{\lambda}_1 + 2\tilde{\mu}_1) + k_{\phi_2}(\tilde{\lambda}_2 + 2\tilde{\mu}_2)}{k_{\phi_1}(\tilde{\lambda}_1 + 2\tilde{\mu}_1) + k_{\phi_2}(\tilde{\lambda}_2 + 2\tilde{\mu}_2)} = \frac{\bar{\rho}_2 \bar{c}_{\phi_2} - \bar{\rho}_1 \bar{c}_{\phi_1}}{\bar{\rho}_2 \bar{c}_{\phi_2} + \bar{\rho}_1 \bar{c}_{\phi_1}}
\tag{4.8a}
$$

and

$$
T_\varphi = \frac{2k_{\phi_1}^2(\tilde{\lambda}_1 + 2\tilde{\mu}_1)}{k_{\phi_2}[k_{\phi_1}(\tilde{\lambda}_1 + 2\tilde{\mu}_1) + k_{\phi_2}(\tilde{\lambda}_2 + 2\tilde{\mu}_2)]} = \frac{2\bar{\rho}_1 \bar{c}_{\phi_2}}{\bar{\rho}_2 \bar{c}_{\phi_2} + \bar{\rho}_1 \bar{c}_{\phi_1}},
\tag{4.8b}
$$

---

[9] Where in component form we have $\hat{\boldsymbol{\sigma}}_1 \mathbf{e}_y = ((\hat{\boldsymbol{\sigma}}_1)_{xy}, (\hat{\boldsymbol{\sigma}}_1)_{yy}, (\hat{\boldsymbol{\sigma}}_1)_{zy})$.

Table 2. Specific equations corresponding to the various acronyms used in the results and discussion of §4d.

acronym	TVA–local TVE	VA–local VE	TVA–rigid	A–rigid	TVE–TVA	VE–VA	TVA–TVE
equation	(4.6) with (4.12)	(4.7) with (4.12)	(B 2) with (B 3)	(B 2) with (B 7)	(4.6) with (4.13)	(4.7) with (4.13)	(4.6) with (4.14)

where we have introduced the free space compressional wave speed in each medium through the relation $\bar{c}_\phi = \bar{\omega}/\bar{k}_\phi$. The well-known equations (4.8) give a clear interpretation of the role of the mechanical impedance $\bar{\rho}\bar{c}_\phi$ when it comes to reflection/transmission, see e.g. §1.4. in [51] (for elasticity). We next discuss the more subtle aspect of the partition of energy at the interface.

(c) Energy partitioning at the interface

Consider the energy flux through the boundary $y = 0$. The average energy flux vectors are defined in (2.27), and since for this problem we have two distinct media, we write[10]

$$\langle \mathbf{J} \rangle = \begin{cases} \langle \mathbf{J}_1 \rangle = -\dfrac{1}{2} \, \mathrm{Re}\{\boldsymbol{\sigma}_1 \dot{\mathbf{u}}_1^* + \theta_1 \mathscr{K}_1 \nabla \theta_1^*\} & \text{for } y \geq 0, \\ \langle \mathbf{J}_2 \rangle = -\dfrac{1}{2} \, \mathrm{Re}\{\boldsymbol{\sigma}_2 \dot{\mathbf{u}}_2^* + \theta_2 \mathscr{K}_2 \nabla \theta_2^*\} & \text{for } y < 0. \end{cases} \tag{4.9}$$

If the boundary conditions (4.5) have been correctly enforced, we expect to have

$$\langle \mathbf{J}_1 \rangle \cdot \mathbf{e}_y = \langle \mathbf{J}_2 \rangle \cdot \mathbf{e}_y \quad \text{at } y = 0, \tag{4.10}$$

meaning that the normal component of the mean energy flux (or power per unit area averaged over a period) is *continuous* across the boundary $y = 0$. It is shown in electronic supplementary material, section SM4 how in order to exploit the role of each mode (4.10) can be written in terms of *energy ratios* for reflected, transmitted and interacting modes with respect to the incident mode, which we write as

$$E_{R_\varphi} + E_{R_\vartheta} + E_{R_\varPhi} + E_{IR_{\mathrm{IR}}} + E_{IR_{\mathrm{RR}}} + E_{T_\varphi} + E_{T_\vartheta} + E_{T_\varPhi} + E_{IT_{\mathrm{TT}}} = 1. \tag{4.11}$$

After solving for all the relevant wave potentials, the above can be used as a check to ensure both numerical accuracy and algebraic correctness. We have noted that the presence of 'crossed terms' (electronic supplementary material, section SM4) represented by interaction coefficients E_{IR}, E_{IT} in (4.11) has been repeatedly ignored in the literature without justification, e.g. [48,49]. We find (not shown) that despite their contribution being small at lower frequencies, their importance in the energy balance equation becomes essential at higher frequencies, and it should therefore be emphasized under what conditions it is a valid approximation to ignore them. Further details can be found in [24] (in the absence of thermal coupling).

(d) Numerical results and discussion

We now present some illustrations of numerical solutions of the general system (4.6) for specific pairs of TVE materials. All results were checked to accurately satisfy the energy flux balance (4.11). We thus demonstrate when thermal or viscous effects are important for these examples, and in particular we can illustrate the effect of stress relaxation. We do this by comparing solutions from the general TVE–TVE case in (4.6) with the solutions of VE–VE (4.7), which ignores thermal effects, the TVA-rigid solutions (B 3), which consider no transmission, and other variations specified in table 2.

We use typical values for air, water, steel and rubber as summarized in table 4. The large parameter space involved allows for an incredibly wide range of materials to be considered. Here

---

[10]Where the product between the Cauchy stress and velocity is written in component form as $\boldsymbol{\sigma}_1 \dot{\mathbf{u}}_1^* = (\boldsymbol{\sigma}_1)_{ij}(\dot{\mathbf{u}}_1)_j^*$ where we sum over j.

we only consider a small fraction of this space, but hope that this work enables further exploration in the future. In particular, we stress that the general TVE framework allows general materials to be considered and no distinction to be required between fluids or solids, etc. which frequently hampers progress via the necessary use of distinct notation for each medium.

(i) Thermo-visco-acoustic-local thermo-visco-elastic: thermo-visco-elastic effects and fluid-structure interaction

In this first instance, we restrict the material parameters of medium 1 to those of air/water whereas for medium 2 we will concentrate on steel/rubber. Both air and water have many applications, while investigating steel and rubber means we are considering both soft and hard solids. We first investigate the use of TVA in medium 1 (or local TVE with $\mu_1 = 0$) and local TVE in medium 2 such that the complex moduli appearing in (4.6) are given by

$$\tilde{\mu}_1(i\omega) = -i\omega\eta_{\mu_1}, \quad \tilde{\lambda}_1(i\omega) = \lambda_1 - i\omega\eta_{\lambda_1}, \quad \tilde{\mu}_2(i\omega) = \mu_2 - i\omega\eta_{\mu_2}, \quad \tilde{\lambda}_2(i\omega) = \lambda_2 - i\omega\eta_{\lambda_2}, \quad (4.12)$$

as discussed in §§2c(iii), 3a. For some parameters, it is difficult to find numerical values in the literature, take for example η_{λ_2} [38]. In these cases, we attempt to use reasonable values based on similar materials. The viscoelastic parameters for steel are taken from table 6.2.2. in [24].

Air–solid interface. Thermal effects are known to be important in air, as we can clearly see in figure 5a, where various reflection coefficients are compared. This is evidenced by the value of thermo-mechanical coupling term for air (second of 3.3b) given by $|L_\theta| \approx 1$ due to air's high thermal expansion coefficient. The pressure dominated reflection coefficient R_φ (responsible for most of the energy) is clearly different for a system which does not include thermal effects in air, such as VA–VE. This is especially true at higher frequencies, in agreement with [5] for narrow slits. Here thermal effects for air are less pronounced for lower frequencies, as shown in figure 5b for $f = 10$ kHz. The reflected shear wave is no longer excited and $|R_\varphi|$'s minimum moves closer to the grazing angle of incidence $\psi = 0$. This behaviour is due to viscous and thermal boundary layer effects near the interface, and can be described through an analytical expression for the *specific admittance*, where the influence of frequency and angle of incidence become apparent, see e.g. §3.2.1 in [7]. Naturally, the solution to the A-Rigid configuration in the absence of any losses gives $R_\varphi = 1$ everywhere, independently of the incident frequency, see (B 7).

Note that neither thermal nor viscous effects are important in medium 2, as using the rigid boundary conditions, TVA-rigid, accurately recovers the reflection coefficient of TVA–TVE. For all of these parameters we obtained almost identical results when swapping rubber for steel, noting that for air–steel the small discrepancy between TVA-rigid and TVA–TVE observed near grazing in figure 5b disappears. The overall excellent agreement is because in both cases there is little transmission into the solid. The same cannot be said of a water–solid interface as we now describe.

Water–solid interface. As the mechanical impedance of water is closer to the impedance of most solids, more mechanical energy will be transmitted into the solid giving rise to fluid–structure interaction (FSI) effects. This is apparent from figure 5c,d where the TVA-rigid solutions no longer agree with the TVA-TVE system. On the other hand, in contrast to air, thermal effects are no longer particularly important, indicated by the fact that TVA–TVE and VA–VE solutions are almost the same. This is due to the smaller thermal coupling for water $|L_\theta| \approx 0.078$. We observe that the $|R_\varphi|$ behaviour for water–Rubber 2 is indistinguishable at low and high frequencies, resembling the purely elastic solutions ((4.7) with $\eta_{\mu_1}, \eta_{\mu_2}, \eta_{\lambda_1}, \eta_{\lambda_2} = 0$) which are independent of frequency. The same can be said for the transmitted modes. Nevertheless, we will observe shortly how this behaviour can change when stress relaxation is considered.

For water-steel the frequency dependence is nevertheless apparent. In the TVA–TVE solutions, boundary layer effects are visible near grazing incidence at higher frequencies (figure 5c), in contrast to the lower frequency regime, where $|R_\varphi|$ remains very close to one as seen in figure 5d. The TVA-Rigid solutions greatly overestimate these effects near $\psi = 0$ at both frequencies. As opposed to the in-air case, reflected boundary layer shear waves into the water were not found,
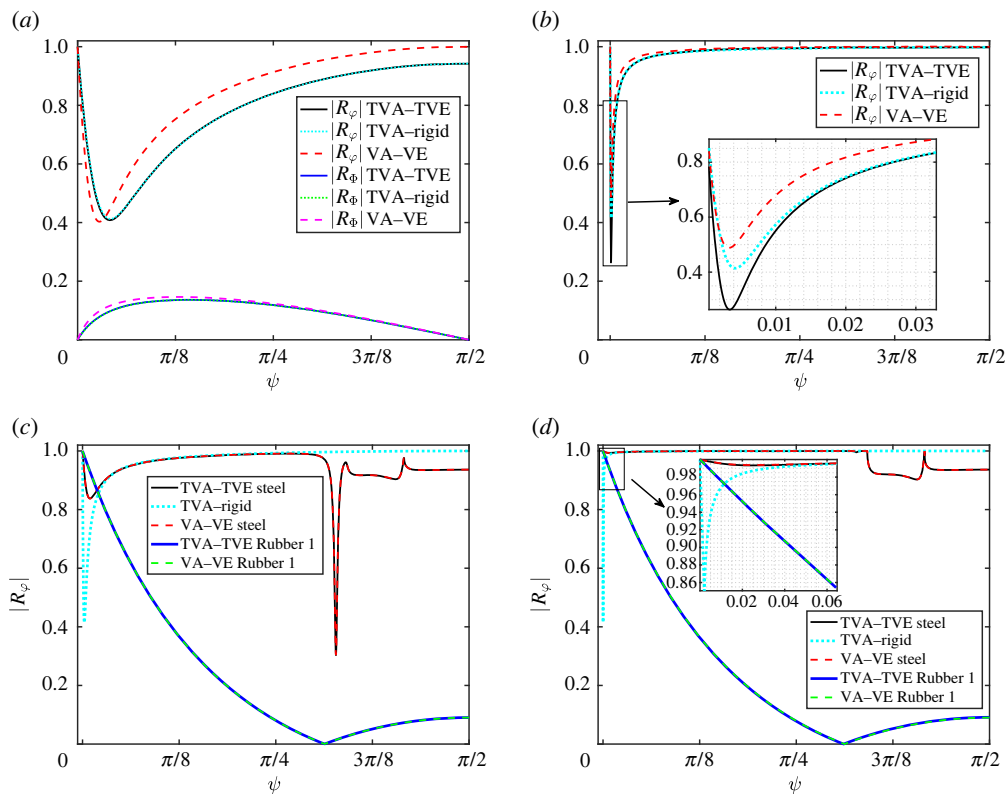
Figure 5. Magnitude of the reflection coefficients as predicted by the different systems in table 2 with the material constants used shown in table 4. The results cover different fluid–solid interfaces for both higher ($f = 10$ MHz) and lower ($f = 10$ MHz) frequencies, and the x-axis shows the angle of incidence ψ. (a) Air–Rubber 2 $f = 10$ MHz, (b) air–Rubber 2 $f = 10$ MHz, (c) water–Rubber 1/steel $f = 10$ MHz, (d) water–Rubber 1/steel $f = 10$ MHz. (Online version in colour.)

i.e. $|R_\Phi| \approx 0$ in each case and hence not included in the figures. The other notable frequency-dependent feature for water–steel is the emergence of a significant reduction in amplitude at high frequencies for a narrow range of angles of incidence around the interval $(\pi/4, 3\pi/8)$. This phenomenon was first observed experimentally in the 1960s for water–aluminum and it was noticed that it disagreed with predictions of elastic reflection–refraction theory. It has been discussed by several authors since including [24,28,47], where the latter reference provides a detailed explanation under a VA–VE model. Under the framework presented in this work, we have extended their model to include thermal losses in both media, although as we can observe these are not manifested in the solutions when compared to the isothermal solution. Finally, we note that the $|R_\varphi|$ behaviour for $\psi \in (3\pi/8, \pi/2)$ in figure 5c,d is elastic and independent of frequency, and the two distinct features in this region are a consequence of the transmitted SV and P waves in the lower half-space being induced, respectively (not shown).

(ii) Influence of stress relaxation

We now explore the effect of stress relaxation in the solid. Little discussion is found on stress relaxation times for metals in the literature since in most instances they are nearly undamped materials, e.g. [15], so here we focus on results for rubbery media following the values in table 4.

Rubber–air interface. We first investigate a TVE–TVA interface, where the incident energy arises from the solid. Following the discussion in §2c(ii), we assume that the relaxation is purely in shear and is governed by a single-term Prony series, with the bulk modulus being a real-valued

Table 3. Shear modulus and Poisson's ratio values according to the SLSM for various values of ωt_r covering the rubbery, transition and glassy regions of the two types of rubbers in consideration.

modulus ωt_r	$\tilde{\mu}$ (MPa) Rubber 1/Rubber 2	$\tilde{\nu}$ Rubber 1/Rubber 2
0.062	$0.338 - 0.607i/21 - 17i$	$0.4999 + 0.00018i/0.489 + 0.008i$
1.005	$5.2 - 4.85i/160 - 140i$	$0.498 + 0.00142i/0.42 + 0.06i$
62.83	$9.99 - 0.154i/299 - 4.4i$	$0.497 + 0.00004i/0.36 + 0.0018i$

Table 4. Thermo-viscous parameter values for air, water, steel and rubber employed in the several plots of §4. Air is taken from [42] and water from engineeringtoolbox. The VE values for steel are taken from table 6.2.2. in [24], which follow from experiments. The high value of η_μ arises from 'fitting' a Kelvin–Voigt model to the imaginary part of the shear modulus which comes from measurements at 10 MHz. The values of rubber are based on the ranges provided in [52].

| TVE parameter values				
parameter (symbol) [unit]	air	water	steel	Rubbers 1 and 2
elastic				
background density (ρ_0) [kg m^{-3}]	1.19	1000	7932	1522 & 2300
isothermal bulk modulus (K) [Pa]	100.72×10^3	2.2×10^9	1.57×10^{11}	1.7×10^9 and 10^9
shear modulus (μ_0) [Pa]	0	0	7.83×10^{10}	10^7 and 3×10^8
relaxed shear modulus for SLSM (μ_∞) [Pa]	—	—	—	3×10^5 and 2×10^7
local viscous				
dynamic shear viscosity (η_μ) [Pa s]	1.8×10^{-5}	10^{-3}	15	10^{-2}
dynamic bulk viscosity (η_K) [Pa s]	1.1×10^{-5}	3×10^{-3}	10^{-8}	10^{-2}
thermal				
thermal conductivity ($\mathcal{K}$) [W m^{-1} K^{-1}]	0.026	0.597	30	2
specific heat at constant pressure (c_p) [J kg^{-1} K^{-1}]	1005	4181.6	500	1300
ambient temperature (T_0) [K]	300	300	300	300
coefficient of thermal expansion (α) [K^{-1}]	1/300	2.6×10^{-4}	1.7×10^{-5}	2.5×10^{-4}
ratio of specific heats (γ) [—]	1.39	1.01	1.0003	1.008

constant such that

$$\tilde{\mu}_1(i\omega) = \mu_{\infty_1} - (\mu_{0_1} - \mu_{\infty_1})\frac{i\omega t_r}{1 - i\omega t_r}, \quad \tilde{\lambda}_1(i\omega) = K_1 - \frac{2}{3}\tilde{\mu}_1(i\omega) \tag{4.13a}$$

and

$$\tilde{\mu}_2(i\omega) = -i\omega\eta_{\mu_2}, \quad \tilde{\lambda}_2(i\omega) = \lambda_2 - i\omega\eta_{\lambda_2}. \tag{4.13b}$$

As discussed in §2c(ii), the relevant non-dimensional parameter to investigate the different regions of the modulus is ωt_r. For a given material, the relaxation time is fixed and it scales the resulting frequency behaviour. Here we choose three distinct values, namely $\omega t_r = 0.063, 1.005, 62.83$ corresponding to the rubbery, transition and glassy regions of the shear modulus, as shown explicitly in table 3.

For Rubber 1 in table 4, it was found that $R_\varphi \approx -1$, independently of $\psi, \omega t_r$. This is due to the fact that for Rubber 1 $K_1 \gg |\tilde{\mu}_1(i\omega)|$ at all frequencies since this material is nearly incompressible, and hence the associated Poisson's ratio remains very close to 1/2 in each case. Nevertheless, for Rubber 2 the situation is much different, as shown in figure 6. In the rubbery region $\omega t_r = 0.063$,
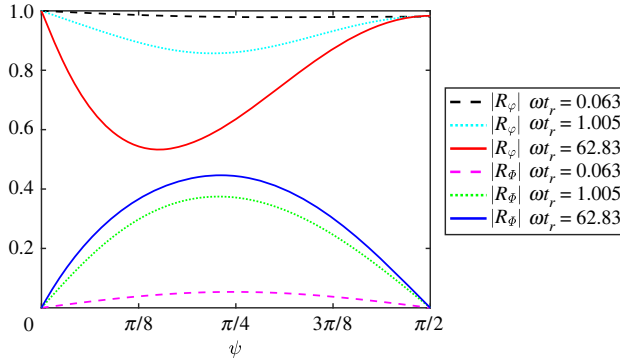
Figure 6. Reflection coefficients for a Rubber 2–air interface in the rubbery, transition and glassy regions of the shear modulus according to the SLSM. The material constants used are shown in table 4. (Online version in colour.)

the incident angle dependence on reflection remains small but this changes in the transition region and especially in the glassy region. For $\omega t_r = 62.83$ we observe that the reflected SV wave gets excited with a global maximum near $\psi = \pi/4$ where the amplitude R_Φ becomes almost 50% of that of the incident wave. Despite the smaller ratio μ_{0_1}/μ_{∞_1} of Rubber 2 compared to Rubber 1, its higher magnitude implies that it becomes more compressible and Poisson's ratio reduces (table 3) which in turn excites the reflected shear wave, e.g. for $\omega t_r = 1.005$, we have $|\tilde{v}(i\omega)| = 0.425$. Since these solutions are mainly influenced by Poisson's ratio, for a practical realization it is the frequency dependence $\tilde{v}(i\omega)$ that should be studied more in depth, see e.g. [34] for an extensive review.

For both rubbers, the thermo-mechanical coupling is small such that $L_\theta = O(10^{-2})$, and therefore equivalent results are obtained when using the VE–VE system (4.7). Again due to the mechanical impedance mismatch, transmission into the air is negligible. In fact, these results obtained for air in the lower medium had excellent agreement with the associated problem of a single TVE half-space with traction free and isothermal/adiabatic boundary conditions. Although not included in this report, these simpler solutions showcase explicitly the role of v described above (see e.g. §5.6 in [51] in the absence of losses).

Fluid–rubber interface. In the second example, we want to investigate whether stress relaxation effects in rubber can still alter the reflection/transmission pattern when the incident energy comes from the fluid, so we return to a fluid–solid TVA–TVE interface such that

$$\tilde{\mu}_1(i\omega) = -i\omega\eta_{\mu_1}, \quad \tilde{\lambda}_1(i\omega) = \lambda_1 - i\omega\eta_{\lambda_1} \tag{4.14a}$$

and

$$\tilde{\mu}_2(i\omega) = \mu_{\infty_2} - (\mu_{0_2} - \mu_{\infty_2})\frac{i\omega t_r}{1 - i\omega t_r}, \quad \tilde{\lambda}_2(i\omega) = K_2 - \frac{2}{3}\tilde{\mu}_2(i\omega). \tag{4.14b}$$

In the case of air–Rubber (1 and 2), for each value of ωt_r the reflected modes behave as discussed with the local TVE model in figure 5a,b and the transmission into the rubber is negligible. Although as we observed in figure 5c, energy gets transmitted into the solid in a water–Rubber 1 interface, the frequency variation of the shear modulus according to the SLSM did not manifest in any results that deviated much from the Local TVE case. This occurs due to the high Poisson's ratio of Rubber 1, as discussed above for the rubber–air interface. For water–Rubber 2 however, significant differences in $|R_\varphi|$, $|T_\varphi|$, $|T_\Phi|$ do arise.

It is often of interest in application to avoid any acoustic reflection in the incident medium, which requires impedance matching with the neighbouring medium. Since for these materials thermal coupling was found to be unimportant, (4.8) can be used to tune Rubber 2 in order to impedance match it with the water for a particular value of frequency. As an illustration, following this principle we simply tune the density of Rubber 2 ($\bar{\rho}_2 : 2300 \to 1588 \, \text{kg m}^{-3}$) in
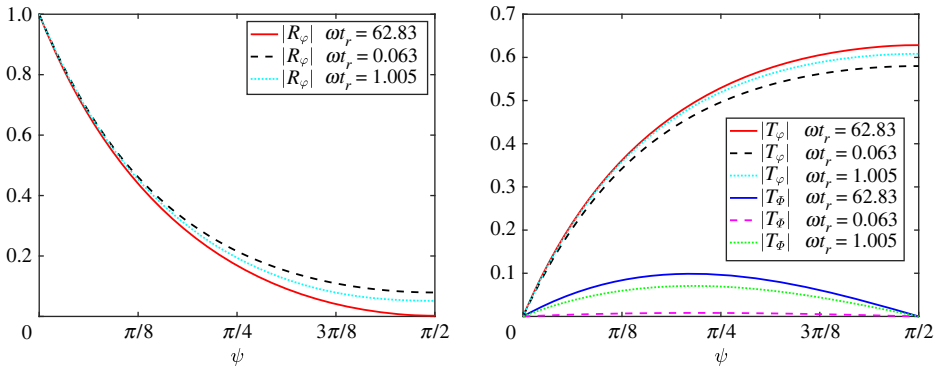
Figure 7. Reflection/transmission of a water–Rubber 2 interface according to (4.6), where the density of material 2 has been adapted to impedance match with μ_0 in the glassy region. (Online version in colour.)

order to impedance match it with water in the glassy region represented by $\omega t_r = 62.83$, as shown in figure 7. For the reflected/transmitted P waves, the differences between ωt_r increase monotonically as ψ moves from grazing to normal incidence, where the maximum difference occurs. A 10% variation in the magnitude of the reflected amplitude was found between the glassy and rubbery regions. Similar values for this variation yield for the transmitted shear wave, where the maximum difference occurs near $\psi = \pi/4$.

5. Conclusion

Understanding how to model and exploit loss mechanisms in complex materials is important in many applications and increasingly so in the areas of composite media and metamaterials science. Here we have presented a general unified framework, permitting the incorporation of both creep and relaxation via time non-locality, with which one can study linear wave propagation in thermo-visco-elastic media. We illustrated the framework with the configuration of two semi-infinite half-spaces in perfect contact, with plane compressional-wave incidence on the interface that separates the media. We used this example to compare solutions when incorporating viscosity and thermal effects. For FSI effects we noted the important role of the incident frequency and angle on the contribution to visco-thermal effects as well as visco-elastic attenuation within the solid. For the latter, we emphasized the differences induced when the shear modulus includes stress relaxation, as opposed to the local-in-time counterpart where the real part of the modulus remains fixed.

There are many advantages to the unified framework presented here, but three are key. Firstly, it provides a mechanism to study canonical wave propagation problems when there is coupling between different media, and specifically between what are classically perceived as *fluid* and *solid*. As we have shown this distinction is often clear away from boundaries but is less clear close to such interfaces. A unified framework allows such modelling to be carried out once and for all, without the need to develop separate models for each, as is often done [5,6]. To help illustrate the connection between the framework and other well-known models for dissipation, such as thermo-visco-acoustics in fluids, or visco-elasticity, we have demonstrated how to take the appropriate limits to recover these special cases from our framework.

The second key advantage is the potential use of the framework to understand fully time-dependent problems. It is common for wave propagation problems to be studied at single frequencies, which is sufficient in its own right, but if a viscoelastic model is employed, one must be confident that this model is capable of representing the behaviour across a broad range of frequencies, especially if one wishes to subsequently use this model in the time domain, given that a time domain signal will encompass a vast range of frequency content in general. It is often

seen as standard practice to employ simple Kelvin–Voigt models to account for visco-elasticity, with 'parameters that are frequency dependent' [14,53]. While this may be sufficient to model the material response at fixed frequencies, it is not sufficient to be employed in the time domain.

The third advantage of the unified framework that incorporates stress relaxation and creep compliance is that one can then employ these models to understand and describe wave propagation in polymeric media. Such materials have the behaviour as illustrated throughout this paper, with a specific frequency at which maximum loss occurs, also related to a temperature, know as the glass-transition. This behaviour is particularly important to accommodate when polymers are employed in the metamaterial context since the design of metamaterials focuses on internal resonance and therefore one may wish to design this resonance with knowledge of this transition in mind, either to increase or decrease inherent attenuation in the material.

We anticipate that the presented framework can now be employed on various problems of interest. In particular, it can be used to unify the approach to the problem described in [5] and this will be extended in upcoming work.

Appendix A. Local isotropic TVE stress–strain and entropy relations

By assuming that the free energy Ψ can be written as a function of the strain ε and temperature T and given its relationship with the Cauchy stress (2.5), the strain energy can be written explicitly as a series expansion about $\varepsilon = \mathbf{0}$ and $T = T_0$, up to second order in ε, and T. This leads to

$$
\rho_0 \Psi(\varepsilon, T) = \rho_0 \left(\Psi|_{\varepsilon=\mathbf{0},T=T_0} + \left.\frac{\partial \Psi}{\partial \varepsilon}\right|_{\mathbf{0},T_0} : \varepsilon + \left.\frac{\partial \Psi}{\partial T}\right|_{\mathbf{0},T_0} (T - T_0) + \frac{1}{2!}\varepsilon : \left.\frac{\partial^2 \Psi}{\partial \varepsilon \partial \varepsilon}\right|_{\mathbf{0},T_0} : \varepsilon \right.
$$
$$
\left. + \left.\frac{\partial^2 \Psi}{\partial T^2}\right|_{\mathbf{0},T_0} \frac{(T - T_0)^2}{2!} + 2\frac{(T - T_0)}{2!} \left.\frac{\partial^2 \Psi}{\partial \varepsilon \partial T}\right|_{\mathbf{0},T_0} : \varepsilon \right), \tag{A 1}
$$

where we have assumed that $\varepsilon, (T - T_0)/T_0 \ll 1$ and both are of the same order. If we further assume isotropy, we can reach

$$
\rho_0 \left.\frac{\partial \Psi}{\partial \varepsilon}\right|_{\mathbf{0},T_0} : \varepsilon = a_0 \mathrm{tr}(\varepsilon), \qquad \left.\frac{\partial^2 \Psi}{\partial T^2}\right|_{\mathbf{0},T_0} = -\frac{c_v}{T_0} \tag{A 2a}
$$

and

$$
\rho_0 \varepsilon : \left.\frac{\partial^2 \Psi}{\partial \varepsilon \partial \varepsilon}\right|_{\mathbf{0},T_0} : \varepsilon = \lambda (\mathrm{tr}\varepsilon)^2 + 2\mu\, \mathrm{tr}(\varepsilon^2), \qquad \rho_0 \left.\frac{\partial^2 \Psi}{\partial \varepsilon \partial T}\right|_{\mathbf{0},T_0} : \varepsilon = -\alpha K \mathrm{tr}(\varepsilon), \tag{A 2b}
$$

where $K = \lambda + 2\mu/3$ denotes the isothermal bulk modulus, and the material constants $\mu, \lambda, c_v, \alpha, a_0$ have conveniently been chosen to fit standard conventions. Using (2.4), and (A 2) we may rewrite (A 1) as

$$
\rho_0 \Psi(\varepsilon, T) = \rho_0(\mathcal{E}_0 - T_0\mathfrak{s}_0 - \mathfrak{s}_0(T - T_0) - \frac{c_v}{2T_0}(T - T_0)^2) + a_0 \mathrm{tr}\varepsilon
$$
$$
+ \frac{1}{2}(\lambda(\mathrm{tr}\varepsilon)^2 + 2\mu\mathrm{tr}(\varepsilon^2)) - \alpha K(T - T_0)\mathrm{tr}(\varepsilon). \tag{A 3}
$$

From the above, (2.4), and (2.5) it follows that the Cauchy stress tensor and entropy become

$$
\boldsymbol{\sigma} = a_0\boldsymbol{I} + \lambda\mathrm{tr}(\varepsilon)\boldsymbol{I} + 2\mu\varepsilon - \alpha K(T - T_0)\boldsymbol{I} + 2\eta_\mu\dot{\varepsilon} + \left(\eta_K - \frac{2\eta_\mu}{3}\right)\boldsymbol{I}\mathrm{tr}(\dot{\varepsilon}) \tag{A 4a}
$$

and

$$
\mathfrak{s} = \mathfrak{s}_0 + \frac{c_v}{T_0}(T - T_0) + \frac{\alpha K}{\rho_0}\mathrm{tr}\varepsilon. \tag{A 4b}
$$

We can let $a_0 = 0$ since we are not considering any form of pre-stress. By comparing with (2.7), we can now identify: λ and μ as the (isothermal) Lamé coefficients, $c_v = T_0(\partial\mathfrak{s}/\partial T)_{\varepsilon=0}$ as the specific heat at constant deformation (see e.g. Article 1.12 in [18]), and α as the coefficient of volumetric thermal expansion[11] $\alpha = (\partial\mathrm{tr}(\varepsilon)/\partial T)_{\varepsilon=0}$. Equivalent theories for TVE can be derived similarly, in particular if (2.2) is replaced with the Gibbs energy, the specific entropy can be written in terms of stress as (see e.g. [43] equation (34))

$$
\mathfrak{s} = \mathfrak{s}_0 + \frac{\alpha}{3\rho_0}\mathrm{tr}\boldsymbol{\sigma} + c_p\theta, \tag{A 5}
$$

where similarly $c_p = T_0(\partial\mathfrak{s}/\partial T)_{\boldsymbol{\sigma}=0}$ is defined as the specific heat at constant deformation of the solid in consideration. When $\mathrm{tr}(\dot{\varepsilon})$ can be neglected in (A 4a), then we can write (A 4b) in terms of stress to obtain

$$
\mathfrak{s} = \mathfrak{s}_0 + c_v\theta + \frac{\alpha}{3\rho_0}\left(\mathrm{tr}\boldsymbol{\sigma} + 3\alpha K(T - T_0)\right), \tag{A 6}
$$

which can be directly equated with (A 5) in order to obtain the identity (2.11).

Appendix B. Non-dimensionalization and convenient physical limits

(a) Non-dimensionalization

For the numerical implementation, it is convenient to re-write the dimensional equations with non-dimensional quantities. We choose to non-dimensionalize with respect to the thermo-elastic quantities from (the top) medium 1. In particular, we choose $\bar{c}_1$ to denote the (adiabatic) longitudinal speed of sound of the upper material in the lossless case, i.e. $\bar{c}_1^2 = (\bar{\lambda}_1 + 2\bar{\mu}_1)/\bar{\rho}_1$ and $\bar{\ell}$ represents an arbitrary length scale. In order to distinguish between dimensional/non-dimensional quantities here, we write all dimensional quantities with an overbar.

$$
\nabla = \bar{\ell}\overline{\nabla}, \quad \omega = \frac{\bar{\ell}}{\bar{c}_1}\bar{\omega}, \ \{\mathbf{u}_m, \mathbf{x}\} = \frac{1}{\bar{\ell}}\{\bar{\mathbf{u}}_m, \bar{\mathbf{x}}\}, \ \{\phi_m, \varphi_m, \vartheta_m, \Phi_m\} = \frac{1}{\bar{\ell}^2}\{\bar{\phi}_m, \bar{\varphi}_m, \bar{\vartheta}_m, \bar{\Phi}_m\},
$$

$$
\mathscr{K}_m = \frac{\bar{T}_1\bar{\mathscr{K}}_m}{\bar{\rho}_1\bar{c}_1^3\bar{\ell}}, \quad c_{v_m} = \frac{\bar{T}_1}{\bar{c}_1^2}\bar{c}_{v_m}, \quad \alpha_m = \bar{\alpha}_m\bar{T}_1, \ \{\eta_{\lambda_m}, \eta_{\mu_m}\} = \frac{1}{\bar{\rho}_1\bar{c}_1\bar{\ell}}\{\bar{\eta}_{\lambda_m}, \bar{\eta}_{\mu_m}\},
$$

---

[11]Note that for an isotropic material, this term is three times the coefficient of linear thermal expansion, which is also commonly found in the thermodynamic literature.

$$\{\tilde{\lambda}_m, \tilde{\mu}_m, \tilde{K}_m, \boldsymbol{\sigma}_m\} = \frac{1}{\bar{\rho}_1 \bar{c}_1^2} \{\bar{\tilde{\lambda}}_m, \bar{\tilde{\mu}}_m, \bar{\tilde{K}}_m, \bar{\boldsymbol{\sigma}}_m\}, \quad \{k_{\theta_m}^2, k_{\phi_m}^2, k_{\Phi_m}^2, L_{\phi_m}\} = \bar{\ell}^2 \{\bar{k}_{\theta_m}^2, \bar{k}_{\phi_m}^2, \bar{k}_{\Phi_m}^2, \bar{L}_{\phi_m}\},$$

$$k_{\theta_1}^2 = \frac{\mathrm{i}\omega c_{v_1}}{\mathscr{K}_1}, \quad k_{\phi_1}^2 = \frac{\omega^2}{\tilde{\lambda}_1 + 2\tilde{\mu}_1}, \ k_{\Phi_1}^2 = \frac{\omega^2}{\tilde{\mu}_1}, \ L_{\phi_1} = \frac{\mathrm{i}\alpha_1\omega K_1}{\mathscr{K}_1}, \ L_{\theta_1} = -\frac{\alpha_1 K_1}{\tilde{\lambda}_1 + 2\tilde{\mu}_1},$$

$$k_{\theta_2}^2 = \frac{\mathrm{i}\omega c_{v_2}}{\mathscr{K}_2} r, \quad k_{\phi_2}^2 = \frac{\omega^2}{\tilde{\lambda}_2 + 2\tilde{\mu}_2} r, \ k_{\Phi_2}^2 = \frac{\omega^2}{\tilde{\mu}_2} r, \ L_{\phi_2} = \frac{\mathrm{i}\alpha_2\omega K_2}{\mathscr{K}_2}, \ L_{\theta_2} = -\frac{\alpha_2 K_2}{\tilde{\lambda}_2 + 2\tilde{\mu}_2} \left(\frac{\bar{T}_2}{\bar{T}_1}\right),$$

where $m = 1, 2$ depending on the medium, $r = \bar{\rho}_2/\bar{\rho}_1$ is the contrast parameter and the background temperature ratio $\bar{T}_2/\bar{T}_1 = 1$ due to continuity of temperature across the boundary.

(b) TVE–TVE scattering system

This matrix system and its derivation is provided in an open access Mathematica file in [50].

(c) VE–VE scattering system

In §3b, we learned how to recover the theory of isothermal visco-elasticity (VE) from that of TVE. For completeness purposes, we next formulate the scattering problem in §4 for such media. This problem is well discussed in the VE literature, see e.g. [24] §5.3. Equations (4.1)–(4.5) are replaced by

$$\phi_{\mathrm{I}} = \mathrm{e}^{-\mathrm{i}k_{\phi_1}(x\cos\psi + y\sin\psi)}, \quad \psi \in [0, \pi], \tag{B 1a}$$

$$\phi_{\mathrm{R}} = R_\phi \mathrm{e}^{\mathrm{i}k_{\phi_1}\sin\psi\, y}\mathrm{e}^{-\mathrm{i}k_{\phi_1}x\cos\psi}, \quad \phi_{\mathrm{T}} = T_\phi \mathrm{e}^{-\mathrm{i}d_{\Phi_{\mathrm{T}}} y}\mathrm{e}^{-\mathrm{i}k_{\phi_1}x\cos\psi}, \tag{B 1b}$$

and

$$\Phi_{\mathrm{R}} = \mathbf{e}_z R_\Phi \mathrm{e}^{\mathrm{i}d_{\Phi_{\mathrm{R}}} y}\mathrm{e}^{-\mathrm{i}k_{\phi_1}x\cos\psi}, \quad \Phi_{\mathrm{T}} = \mathbf{e}_z T_\Phi \mathrm{e}^{-\mathrm{i}d_{\Phi_{\mathrm{T}}} y}\mathrm{e}^{-\mathrm{i}k_{\phi_1}x\cos\psi}, \tag{B 1c}$$

and $d_{\Phi_{\mathrm{T}}} = \mathrm{i}\sqrt{-(k_{\Phi_2}^2 - k_{\phi_1}^2\cos^2\psi)}$, $d_{\Phi_{\mathrm{R}}} = \mathrm{i}\sqrt{-(k_{\Phi_1}^2 - k_{\phi_1}^2\cos^2\psi)}$ and $d_{\Phi_{\mathrm{T}}} = \mathrm{i}\sqrt{-(k_{\Phi_2}^2 - k_{\phi_1}^2\cos^2\psi)}$, ensures that $\mathrm{Im}\, d_{\Phi_{\mathrm{T}}}, \mathrm{Im}\, d_{\Phi_{\mathrm{R}}}, \mathrm{Im}\, d_{\Phi_{\mathrm{T}}} \geq 0$. The BCs reduce to $\hat{\mathbf{u}}_1^{\mathrm{VE}} = \hat{\mathbf{u}}_2^{\mathrm{VE}}$ and $\hat{\boldsymbol{\sigma}}_1^{\mathrm{VE}}\mathbf{e}_{\mathbf{y}} = \hat{\boldsymbol{\sigma}}_2^{\mathrm{VE}}\mathbf{e}_{\mathbf{y}}$ which must hold on $y = 0$. The application of these four BCs will determine the unique four constants $\{R_\phi, T_\phi, R_\Phi, T_\Phi\}$, see equation (5.3.21) in [24] or [50] for explicit details.

(d) Thermo-visco-elastic-rigid scattering problem

In §3a, we discussed how local TVE yields the classical TVA theory for fluids in the limit of vanishing shear modulus, so we let $\mu \to 0$. For a thermo-viscous fluid in contact with a rigid interface at $y = 0$, we impose no-slip and for the temperature field an isothermal boundary condition, that is $-\mathrm{i}\omega\mathbf{u}^{\mathrm{TVA}} = 0$ and $\theta^{\mathrm{TVA}} = 0$ on $y = 0$, noting that we have dropped the subscript since here we are only considering motion on $y \geq 0$. Following (4.2) our fields are given by

$$\varphi = \mathrm{e}^{-\mathrm{i}k_\varphi x\cos\psi}(\mathrm{e}^{-\mathrm{i}k_\varphi y\sin\psi} + R_\varphi \mathrm{e}^{\mathrm{i}k_\varphi y\sin\psi}) \tag{B 2a}$$

and

$$\vartheta = R_\vartheta \mathrm{e}^{-\mathrm{i}k_\varphi x\cos\psi + \mathrm{i}d_\vartheta y}, \quad \Phi = R_\Phi \mathrm{e}^{-\mathrm{i}k_\varphi x\cos\psi + \mathrm{i}d_\Phi y}, \tag{B 2b}$$

with $d_\vartheta = \mathrm{i}\sqrt{-(k_\vartheta^2 - k_\varphi^2\cos^2\psi)}$, $d_\Phi = \mathrm{i}\sqrt{-(k_\Phi^2 - k_\varphi^2\cos^2\psi)}$ which ensures $\mathrm{Im}\, d_\vartheta, \ \mathrm{Im}\, d_\Phi \geq 0$. Substitution of (B 2) into the governing equations (2.18b), (2.23) and using (2.17), (2.18a) for the boundary conditions given above (B 2), we obtain exact expressions

$$\begin{pmatrix} R_\varphi \\ R_\vartheta \\ R_\Phi \end{pmatrix} = \begin{pmatrix} \dfrac{-\cos^2\psi + \mathcal{B}(\mathcal{F} + \mathcal{G})}{\cos^2\psi - \mathcal{B}(\mathcal{F} - \mathcal{G})} \\ \dfrac{-2\sin\psi\,\mathcal{F}}{\cos^2\psi - \mathcal{B}(\mathcal{F} - \mathcal{G})}\dfrac{k_\varphi}{d_\vartheta} \\ \dfrac{\sin 2\psi}{\cos^2\psi - \mathcal{B}(\mathcal{F} - \mathcal{G})} \end{pmatrix}, \tag{B 3}$$

where

$$\mathcal{B} = \sqrt{\frac{k_\Phi^2}{k_\varphi^2} - \cos^2 \psi}, \quad \mathcal{F} = \frac{d_\vartheta \mathscr{T}_\varphi}{k_\varphi(\mathscr{T}_\vartheta - \mathscr{T}_\varphi)}, \; \mathcal{G} = \frac{\mathscr{T}_\vartheta \sin \psi}{\mathscr{T}_\vartheta - \mathscr{T}_\varphi}. \tag{B 4}$$

With the current potentials (B 2), the energy balance in this case reduces to

$$E_{R_\varphi} + E_{R_\vartheta} + E_{R_\Phi} + E_{IR_{IR}} + E_{IR_{RR}} = 1, \tag{B 5}$$

which are defined in electronic supplementary material, section SM4 and we must use the current potentials (B 2). The visco-acoustic VA solution can be directly obtained from (B 3), (B 4) by letting $\mathscr{T}_\varphi \to 0$ which results in $\mathcal{F} \to 0$ and $\mathcal{G} \to \sin \psi$ so that (B 3) becomes

$$R_\varphi \to \frac{-\cos^2 \psi + \mathcal{B} \sin \psi}{\cos^2 \psi + \mathcal{B} \sin \psi}, \quad R_\vartheta, \to 0, \; R_\Phi \to \frac{\sin 2\psi}{\cos^2 \psi + \mathcal{B} \sin \psi}. \tag{B 6}$$

Finally, for the purely acoustic solution in the absence of any losses, we must further let $\eta_\mu \to 0$, which results in $\mathcal{B} \to \infty$, obtaining only the trivial solution

$$R_\varphi \to 1, \quad R_\vartheta, \; R_\Phi \to 0. \tag{B 7}$$

References

1. Tobolsky AV, McLoughlin JR. 1952 Elastoviscous properties of polyisobutylene. V. The transition region. *J. Polymer Sci.* **8**, 543–553. (doi:10.1002/pol.1952.120080512)
2. Obaid N, Kortschot MT, Sain M. 2017 Understanding the stress relaxation behavior of polymers reinforced with short elastic fibers. *Materials* **10**, 472. (doi:10.3390/ma10050472)
3. Jeong YH. 1987 Frequency-dependent shear modulus of glycerol near the glass transition. *Phys. Rev. A* **36**, 766. (doi:10.1103/PhysRevA.36.766)
4. Kari L, Eriksson P, Stenberg B. 2001 Dynamic stiffness of natural rubber cylinders in the audible frequency range using wave guides. *Kautsch. Gummi Kunstst.* **54**, 106–106.
5. Cotterill PA, Nigro D, Abrahams ID, Garcia-Neefjes E, Parnell WJ. 2018 Thermo-viscous damping of acoustic waves in narrow channels: a comparison of effects in air and water. *J. Acoust. Soc. Am.* **144**, 3421–3436. (doi:10.1121/1.5078528)
6. Karlsen JT, Bruus H. 2015 Forces acting on a small particle in an acoustical field in a thermoviscous fluid. *Phys. Rev. E* **92**, 043010. (doi:10.1103/PhysRevE.92.043010)
7. Bruneau M. 2013 *Fundamentals of acoustics*. New York, NY: John Wiley & Sons.
8. Cummer SA, Christensen J, Alù A. 2016 Controlling sound with acoustic metamaterials. *Nat. Rev. Mater.* **1**, 16001. (doi:10.1038/natrevmats.2016.1)
9. Jiménez N, Romero-García V, Pagneux V, Groby J-P. 2017 Rainbow-trapping absorbers: Broadband, perfect and asymmetric sound absorption by subwavelength panels for transmission problems. *Sci. Rep.* **7**, 13595. (doi:10.1038/s41598-017-13706-4)
10. Pham K, Maurel A, Marigo J-J. 2017 Two scale homogenization of a row of locally resonant inclusions-the case of anti-plane shear waves. *J. Mech. Phys. Solids* **106**, 80–94. (doi:10.1016/j.jmps.2017.05.001)
11. Touboul M, Pham K, Maurel A, Marigo J-J, Lombard B, Bellis C. 2020 Effective resonant model and simulations in the time-domain of wave scattering from a periodic row of highly-contrasted inclusions. *J. Elast.* **142**, 53–82. (doi:10.1007/s10659-020-09789-2)
12. Krushynska AO, Kouznetsova VG, Geers M. 2016 Visco-elastic effects on wave dispersion in three-phase acoustic metamaterials. *J. Mech. Phys. Solids* **96**, 29–47. (doi:10.1016/j.jmps.2016.07.001)
13. Fernández-Marín AA, Jiménez N, Groby J-P, Sánchez-Dehesa J, Romero-García V. 2019 Aerogel-based metasurfaces for perfect acoustic energy absorption. *Appl. Phys. Lett.* **115**, 061901. (doi:10.1063/1.5109084)
14. Favretto-Anrès N, Rabau G. 1997 Excitation of the Stoneley–Scholte wave at the boundary between an ideal fluid and a viscoelastic solid. *J. Sound Vib.* **203**, 193–208. (doi:10.1006/jsvi.1996.0884)
15. Liao Y, Wells V. 2006 Estimation of complex modulus using wave coefficients. *J. Sound Vib.* **295**, 165–193. (doi:10.1016/j.jsv.2005.12.045)

29

royalsocietypublishing.org/journal/rspa *Proc. R. Soc. A* **478**: 20220193

16. Chen T. 2000 Determining a Prony series for a viscoelastic material from time varying strain data, 21p. *NASA*.

17. Marsden JE, Hughes TJR. 1994 *Mathematical foundations of elasticity*. New York, NY: Dover publications.

18. Boley BA, Weiner JH. 2012 *Theory of thermal stresses*. Malabar, FL: Robert E. Krieger Publishing Company.

19. Coleman BD, Noll W. 1963 The thermodynamics of elastic materials with heat conduction and viscosity. *Arch. Ration. Mech. Anal.* **13**, 167–178. (doi:10.1007/BF01262690)

20. Liu I-S. 1972 Method of lagrange multipliers for exploitation of the entropy principle. *Arch. Ration. Mech. Anal.* **46**, 131–148. (doi:10.1007/BF00250688)

21. Ferry JD. 1980 *Viscoelastic properties of polymers*. New York, NY: John Wiley & Sons.

22. Cattaneo C. 1958 A form of heat conduction equation which eliminates the paradox of instantaneous propagation. *Comptes Rendus* **247**, 431–433.

23. Lord HW, Shulman Y. 1967 A generalized dynamical theory of thermoelasticity. *J. Mech. Phys. Solids* **15**, 299–309. (doi:10.1016/0022-5096(67)90024-5)

24. Borcherdt RD. 2009 *Viscoelastic waves in layered media*. Cambridge, UK: Cambridge University Press.

25. Caviglia G, Morro A. 2005 Harmonic waves in thermoviscoelastic solids. *Int. J. Eng. Sci.* **43**, 1323–1336. (doi:10.1016/j.ijengsci.2005.05.013)

26. Graff KF. 2012 *Wave motion in elastic solids*. Oxford, UK: Clarendon Press.

27. Nowacki W. 2013 *Thermoelasticity*. Amsterdam, The Netherlands: Elsevier.

28. Deschamps M, Cheng C. 1989 Liquid-thermoviscoelastic solids interface. *Ultrasonics* **27**, 308–313. (doi:10.1016/0041-624X(89)90073-5)

29. Ieşan D. 2011 On a theory of thermoviscoelastic materials with voids. *J. Elast.* **104**, 369–384.

30. Christensen RM, Naghdi PM. 1967 Linear non-isothermal viscoelastic solids. *Acta Mech.* **3**, 1–12. (doi:10.1007/BF01193596)

31. Christensen RM. 2012 *Theory of viscoelasticity: an introduction*. Amsterdam, The Netherlands: Elsevier.

32. Berjamin H, Destrade M, Parnell WJ. 2021 On the thermodynamic consistency of quasi-linear viscoelastic models for soft solids. *Mech. Res. Commun.* **111**, 103648. (doi:10.1016/j.mechrescom.2020.103648)

33. Hunter SC. 1961 Tentative equations for the propagation of stress, strain and temperature fields in viscoelastic solids. *J. Mech. Phys. Solids* **9**, 39–51. (doi:10.1016/0022-5096(61)90037-0)

34. Tschoegl NW, Knauss WG, Emri I. 2002 Poisson's ratio in linear viscoelasticity–a critical review. *Mech. Time-Dependent Mater.* **6**, 3–51. (doi:10.1023/A:1014411503170)

35. Balbi V, Shearer T, Parnell WJ. 2018 A modified formulation of quasi-linear viscoelasticity for transversely isotropic materials under finite deformation. *Proc. R. Soc. A* **474**, 20180231. (doi:10.1098/rspa.2018.0231)

36. Gottenberg WG, Christensen RM. 1964 An experiment for determination of the mechanical property in shear for a linear, isotropic viscoelastic solid. *Int. J. Eng. Sci.* **2**, 45–57. (doi:10.1016/0020-7225(64)90010-2)

37. Lifshitz JM, Kolsky H. 1965 The propagation of spherically divergent stress pulses in linear viscoelastic solids. *J. Mech. Phys. Solids* **13**, 361–376. (doi:10.1016/0022-5096(65)90037-2)

38. Ivanova EA. 2010 Derivation of theory of thermoviscoelasticity by means of two-component medium. *Acta Mech.* **215**, 261–286. (doi:10.1007/s00707-010-0324-7)

39. Birge NO, Nagel SR. 1987 Wide-frequency specific heat spectrometer. *Rev. Sci. Instrum.* **58**, 1464–1470. (doi:10.1063/1.1139434)

40. Kaliske M, Rothert H. 1997 Formulation and implementation of three-dimensional viscoelasticity at small and finite strains. *Comput. Mech.* **19**, 228–239. (doi:10.1007/s004660050171)

41. Epstein PS, Carhart RR. 1953 The absorption of sound in suspensions and emulsions. I. Water fog in air. *J. Acoust. Soc. Am.* **25**, 553–565. (doi:10.1121/1.1907107)

42. Pierce AD. 1981 *Acoustics: an introduction to its physical principles and applications*, vol. 678. New York, NY: McGraw-Hill.

43. Lubarda VA. 2004 On thermodynamic potentials in linear thermoelasticity. *Int. J. Solids Struct.* **41**, 7377–7398. (doi:10.1016/j.ijsolstr.2004.05.070)

44. Scharstein RW, Davis AMJ. 2007 Acoustic scattering by a rigid elliptic cylinder in a slightly viscous medium. *J. Acoust. Soc. Am.* **121**, 3300–3310. (doi:10.1121/1.2727332)

30

royalsocietypublishing.org/journal/rspa *Proc. R. Soc. A* **478**: 20220193

45. Wu J, Zhu Z. 1995 An alternative approach for solving attenuated leaky rayleigh waves. *J. Acoust. Soc. Am.* **97**, 3191–3193. (doi:10.1121/1.411822)
46. Cegla FB, Cawley P, Lowe MJS. 2005 Material property measurement using the quasi-scholte mode-a waveguide sensor. *J. Acoust. Soc. Am.* **117**, 1098–1107. (doi:10.1121/1.1841631)
47. Becker FL, Fitch CE, Richardson RL. 1970 Ultrasonic reflection and transmission factors for materials with attenuation. Technical report, Battelle-Northwest, Richland, Wash. Pacific Northwest Lab.
48. Tomar SK, Bhagwan J, Steeb H. 2014 Time harmonic waves in a thermo-viscoelastic material with voids. *J. Vib. Control* **20**, 1119–1136. (doi:10.1177/1077546312470479)
49. Das N, De S, Sarkar N. 2020 Reflection of plane waves in generalized thermoelasticity of type III with nonlocal effect. *Math. Methods Appl. Sci.* **43**, 1313–1336. (doi:10.1002/mma.5947)
50. Linear Thermo-Visco-Elasticity GitHub. See https://github.com/arturgower/ LinearThermoViscoElasticity.
51. Achenbach J. 2012 *Wave propagation in elastic solids*, vol. 16. Amsterdam, The Netherlands: Elsevier.
52. AZO Materials Silicone Rubber material parameters. See www.azom.com/properties.aspx? ArticleID=920 (accessed: 29 November 2021).
53. Favretto-Anrès N. 1996 Theoretical study of the Stoneley-Scholte wave at the interface between an ideal fluid and a viscoelastic solid. *Acta Acustica united with Acustica* **82**, 829–838.
54. García Neefjes E, Nigro D, Gower AL, Assier RC, Pinfield VJ, Parnell WJ. 2022 A unified framework for linear thermo-visco-elastic wave propagation including the effects of stress-relaxation. Figshare. (doi:10.6084/m9.figshare.c.6169749)